Stevin Laboratory
Faculty of Civil Engineering and Geosciences
Delft University of Technology

Report 25.5.10-17

December 2010

Shear Capacity of Concrete Beams without Shear Reinforcement under Sustained Loads

Experimental Results

Ir. R. Sarkhosh / Ir. J.A. den Uijl / Dr.ir. C.R. Braam / Prof.dr.ir. J.C. Walraven

Mailing address:
Delft University of Technology (TU-Delft)
Faculty of Civil Engineering and Geosciences
Concrete Structures Group
Stevin Laboratory II
Stevinweg 1
2628 CN Delft
The Netherlands

1

Table of Contents

Preface

Concrete is a multiphase granular material consisting of aggregate particles of various sizes and irregular shape, embedded in hardened cement paste. The physicochemical processes during the hardening of the cement cause air voids, micro cracks and interfacial bond micro cracks. As a consequence of this heterogeneous structure, concrete displays a non-linear and time-dependent deformation response under sustained loading.

A challenging topic was and still is the failure behaviour of concrete beams without shear reinforcement. The behaviour of cracked reinforced concrete panels can now be satisfactorily predicted for monotonic short-term shear loading conditions. In spite of substantial experimental and theoretical efforts in the past, the shear transfer mechanism in concrete in the case of sustained shear loads is not well known.

When a concrete beam is under high sustained load, a flexural cracking pattern appears along the span. Here, various shear-carrying mechanisms may be developed by a beam, e.g. aggregate-interlock and dowel action. These mechanisms induce tensile stresses in concrete near the crack tip and at the level of the reinforcement. Once the tensile strength of the concrete in these regions is reached, the existing flexural cracks propagate in a diagonal direction or new ones are created. The development of the critical shear crack, however, does not necessarily imply the collapse of the member but in case of high sustained loads, the crack length and therefore the crack width will increase.

The aim of this research is to predict the time-dependent mechanical behaviour of cracked concrete beams subjected to sustained shear loads. The results should enable the designer to quantify the failure load (Ultimate load) and deformations and the propagation of the cracks of beams under sustained shear loads.

1. Test programme

1.1. Goals of the tests

Many researchers have been involved in study on shear capacity of concrete beams without shear reinforcement. Only a few of them discussed the time-dependent behaviour of concrete beams. Most of the researches previously done in this field were focused on small concrete samples subjected to direct shear tests or a notched sample with fixed-crack model. Currently there are some opinions about decreasing the shear capacity of concrete beams in case high sustained loads which are never tested, thus not proved. Based on Dutch Code, the concrete strength in long-term loading is 0.85 of short-term strength. As a result, the shear capacity should decrease.

Besides the parameters which influence the shear capacity of the beam, e.g. concrete strength, longitudinal reinforcement, shear span to depth ratio and axial force, there are some other parameters that rule in time dependent behaviour of a concrete beam. These are creep, shrinkage, stress relaxation and ageing of concrete. When a beam is subjected to a high constant load, shear cracks as well as flexural cracks appear in the beam. If the loading continues for a while, the creep effect causes an increasing deflection of the beam in time. This phenomenon leads to the further opening of current shear and flexural cracks as well as an increase of the length of the cracks. On the other hand the effect of stress relaxation causes a reduction of stress at the crack tip and the zone with micro-cracks. Besides that, the increase of concrete strength in time reduces the chance that cracks already present will grow or new cracks arise.

In this project the influence of long-term loading on the shear capacity of concrete beams without web reinforcement is being investigated. The goal is to quantify the possible shear capacity loss due to long-term loading. For that reason several test series will be carried out on concrete beams subjected to high shear loads close to the failure load. The beams will experience this load for a maximum period of half a year. Meanwhile, the deflection, crack growth and cracks width will be monitored. Finally a relation between loading duration, crack width and length, load level and concrete strength will be established.

10 series of concrete beams, each series contains 6 specimens (Totally 60 beams), are intended to cast. The first series is the reference test which is tested only in short-term loading to obtain the approximate shear capacity of the beams and the scatter of the results. Other series are going to be tested in both short-term and long-term loading; in each series, there are 3 beams which are tested in short-term loading to obtain the ultimate shear capacity and 3 beams which are tested in long-term loading ranging from 87% to 97.5% of ultimate shear capacity. Various load levels (87%, 90%, 92.5%, 95% and 97.5% of ultimate capacity) will be applied on the beams subjected to long-term loading. Moreover, two types of concrete strength (Normal strength and high strength) are used in this research to compare their behaviour in long-term loading; series 1-5 are NSC and series 6-10 are HSC.

The main objectives of the experimental research are:

- To study the influence of long-term loading on the shear capacity of beams without shear reinforcement.

- To evaluate the influence of the load level on crack propagation to find out if there is any relation between the level of loading and the shear capacity of a concrete beam.
- To evaluate the rate of crack growth (in width and length) in a concrete beam subjected to a sustained load. In case of sustained loads, the beam experiences the effects of creep, stress relaxation and ageing of the concrete. All these effects should be considered during the tests.
- To compare the behaviour of High Strength Concrete (HSC) beams with Normal Strength Concrete (NSC) beams regarding the crack pattern, crack width and level of loading.
- To propose a time dependent relation for crack width and crack length in concrete beams subjected to sustained loads.

1.2. Design of the specimen

In order to achieve the objectives mentioned before, two types of concrete beams (NSC and HSC) without shear reinforcement are designed and tested. The details of the 3000 mm long × 200 mm wide × 450 mm deep beam specimen which are tested in a 2400 mm span under 3-point bending are explained in section 1.4. The shear span considered to be 1200 mm so the a/d ratio is about 2.9.

The test program consists of 10 series of beams; series 1-5 designed to have normal strength concrete (35 MPa) and series 6-10 designed to have high strength concrete (70 MPa).

The beams should resist bending and only fail in shear. The FE-modelling is done in ATENA software and extra hand calculations are done using Rafla's empirical formula, see Appendix I. It should be noted that Rafla's formula is derived based on the results of normal strength concrete tests.

1.3. Theoretical failure loads

The calculation of the shear resistance of concrete beams based on the actual values of concrete strength is presented in section 4.2.

1.4. Shape and dimensions of beams, layout of reinforcement

In order to perform different levels of loading on two types of concrete (normal and high strength concrete), it is planned to cast 10 series of concrete beams. Each series consists of 6 beams and 36 cubes for compressive test. The dimensions and cross section of the beams are presented in Fig. 1 and Fig. 2.

Table 1: Dimensions of casted beams

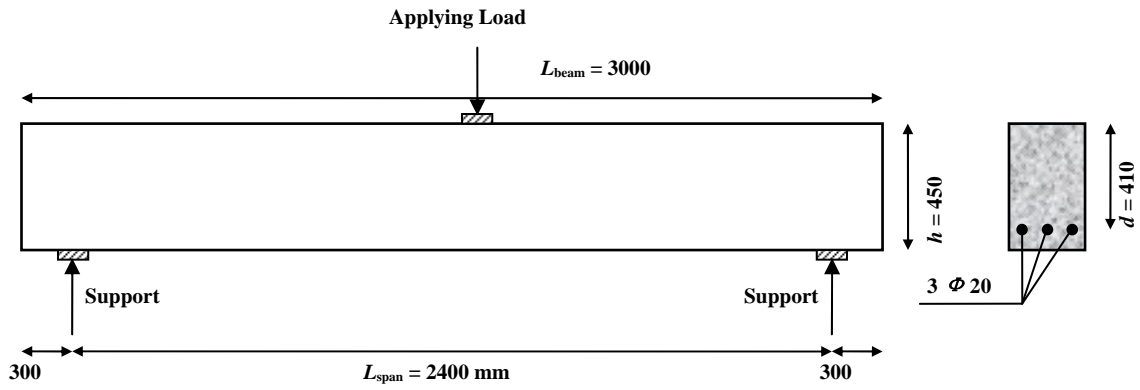| Series No.	h [mm]	b [mm]	d [mm]	L_{beam} [mm]	L_{span} [mm]	Main Reinforcement	Bar spacing [mm]	Reinforcement ratio ρ
1-5	450	200	410	3000	2400	3 Ø 20mm	40	1.05%
6-10	450	200	407	3000	2400	3 Ø 25mm	32	1.63%

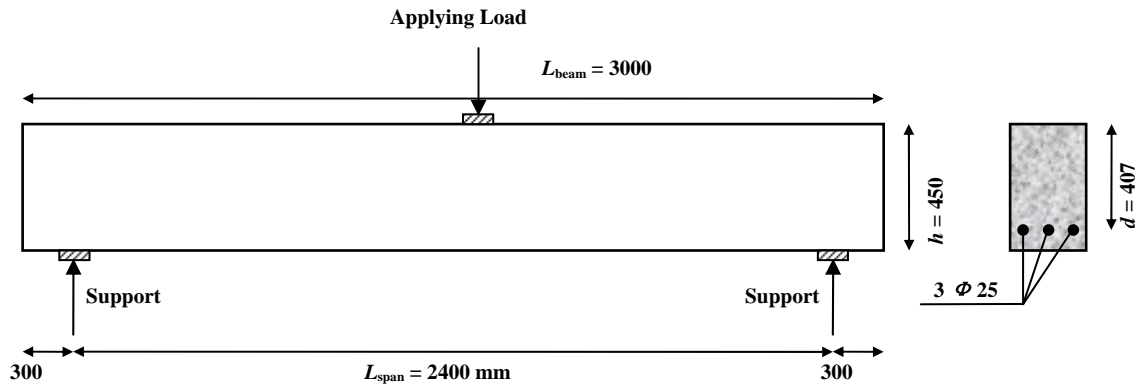**Fig. 1: Dimensions and cross section of the beams in series 1-5**

Fig. 2: Dimensions and cross section of the beams in series 6-10

Reinforcing bars are welded to a steel plate at both ends of the beam. The dimension of steel plates is 100×200×10 mm with a circular cut-out at the position of reinforcements in order to weld at both sides.
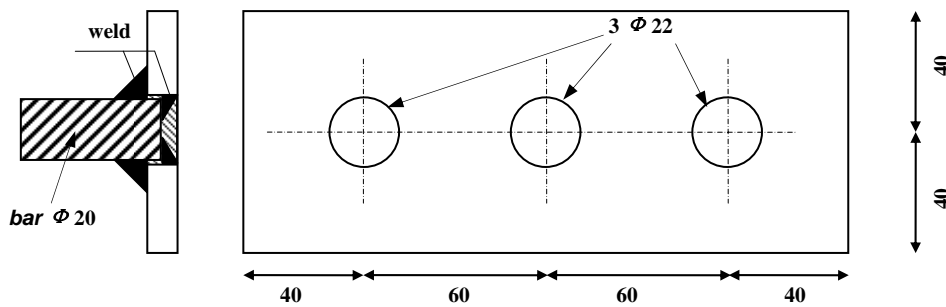
Fig. 3: Layout of end plates for reinforcement in series 1-5

1.5. Material properties

1.5.1. Concrete Mix

Two concrete classes, C28/35 and C53/65, are chosen for normal concrete and high strength concrete respectively. The strength of concrete in each cast was different, (because the concrete was delivered by commercial plant). In casts 1 and 2, the water of the aggregates was not accounted for in the water/cement ratio, thus the strength of the concrete is lower than the

expected value for that concrete class. In cast 5, in order to have the same strength as casts 1 and 2, the concrete class is changed.

The mix for cast 6 and 7 (high strength concrete) contains 280 kg/m^3 Portland Cement type I and 145 kg/m^3 cement type III/B whereas the mix for the normal concrete contained 330 kg cement type III/B. The amount of cement in cast 5 is reduced to 320 kg in the mix to have the same concrete strength as casts 1 and 2. Rounded river aggregates are used in concrete mixture.

General properties of concrete in each series are shown in Table 2. Sieve analysis and concrete mixture are shown in Appendix I.

Table 2. General properties of concrete

Series	Strength Class	Slump	water/cement ratio	Chloride M/M	Temperature
1	C28/35	100-150 mm	0.52	0.20%	20ºC
2	C28/35	100-150 mm	0.52	0.20%	15ºC
3	C28/35	100-150 mm	0.52	0.20%	15ºC
4	C28/35	100-150 mm	0.52	0.20%	10ºC
5	C20/25	100-150 mm	0.540	0.21%	15ºC
6	C53/65	100-150 mm	0.402	0.16%	20ºC
7	C53/65	100-150 mm	0.388	0.16%	23ºC

1.5.2. Steel

Reinforcing bars of 20 mm diameter for series 1-5 and 25 mm diameter for series 6 are used. Three bars at the bottom of the section are required to prevent flexural failure to occur. The bars are welded to the end plate at both ends of a beam.

Tensile tests performed on samples from reinforcing bars show a yield strength of 555 MPa and an ultimate strength of 680 MPa for bars with 20 mm diameter. For bars with 25 mm diameter, a yield strength of 572 MPa and an ultimate strength of 651 MPa is obtained.

1.6. Manufacturing (Preparation/casting/storage) of the specimens

The concrete is delivered by a truck mixer from *Dyckerhoff Basal plant* in Delft. Each beam is cast in four layers and during casting poker vibrators are used to compact the concrete. For standard tests, 36 cubes (150 mm) are cast together with each series of casting. For compacting casts 1-4, small poker vibrators are used. This could be a reason for the large scatter in the results of compressive tests. Therefore, for compacting casts 5-7, a shaking table used with a compacting time of 30 seconds. The beams and cube samples are covered with plastic sheets after casting. For high strength concrete, one day after casting, the surface of the beams is made wet.

After about 10 days, the beams are demoulded and stored in a climate room (RH=50% and T=20ºC). The cubes are demoulded after 1 day and stored in a fog room (RH=99% and T=20ºC).

1.7. Test arrangement and setup

The 3.0 m long beams are loaded in 3-point-bending with a span of 2.40 m. The loading scheme is represented in Fig. 1. The dimensions of the loading plates and supports are 100 mm in horizontal and 200 mm in transverse direction, which covers the width of the beam.

The setup as shown in Fig. 4 consists of a steel frame which holds the concrete beam and loading system inside: a hydraulic actuator that applies the load, an accumulator to keep the oil pressure constant, a load cell between the actuator and a loading plate to measure the load, one loading plate at the middle of the beam with loading area of 100×200 mm, two roller supports each with a contact area of 100×200 mm, one 20 mm LVDT at midspan and a set of 10 mm LVDT's diagonally installed at both sides of the beam symmetrically. Totally 6 test setups with the same equipment are built in the climate room (RH=50% and T=20ºC) and prepared for parallel tests.

All tests are carried out in a load controlled mode. Under load control, the amount of load serves as the primary feedback. The load is applied to the beam by a hand-operated hydraulic jack with 600 bar capacity.

The setup used for series 1-3 has a capacity of 200 kN. Since some of the specimens have a large capacity, the actuators and load cells are replaced to apply a maximum of 400 kN force.
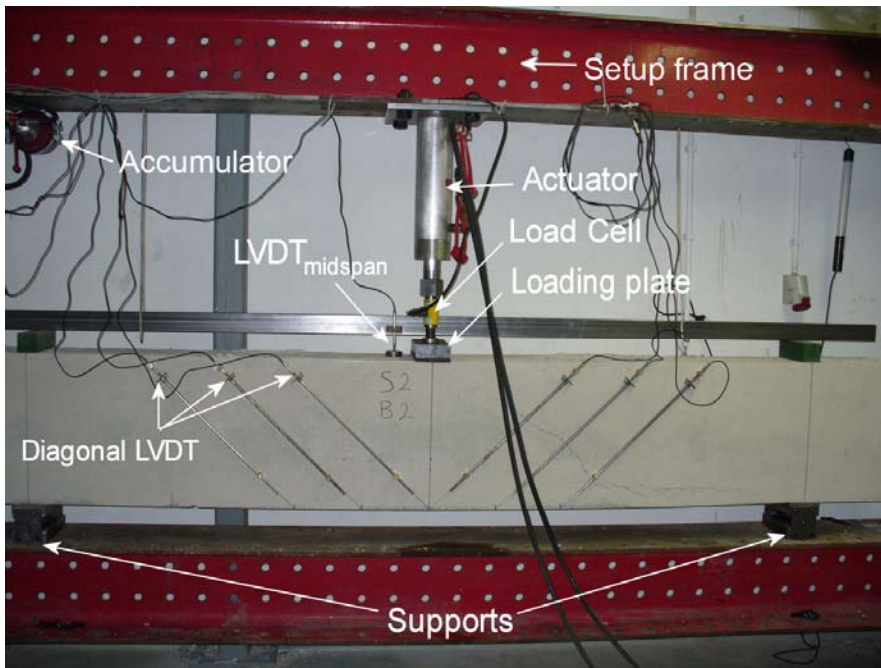

Fig. 4: The setup with capacity up to 200 kN

2. Measuring programme

The measuring system installed on each beam consists of a load-cell, one LVDT at midspan with 20 mm measuring range and two LVDT's with 10 mm measuring range. Extra measuring system with a manually operated LVDT (Measuring range=40-65 mm) is applied on beams with high strength concrete.

The zero measurements are taken when the beams are only loaded by their dead weight. Thus, the influence of the dead load is not incorporated in the measuring results of the LVDT's.

2.1. Load / support reactions

One load cell installed between the actuator and the loading plate is used to measure the applied load, since the tests are in 3-point bending (Fig. 4) with equal distances from that loading plate to the supports at both sides.

2.2. Deflections

The deflection at mid-span is measured relative to the supports with a LVDT at mid-span. To measure deflections accurately, a stiff steel frame which holds the LVDT is fastened at both ends of the beam at the position of the supports. It should be noticed that because of the position of loading plate at mid-span it was hard to install the LVDT exactly at the middle of the beam. Therefore the LVDT installed at 100 mm distance to mid-span (to the left in Fig. 4).

2.3. Crack widths and crack propagation

In order to measure the shear crack width, two diagonal LVDT's are used at left and right sides. The positions of the LVDT's at both sides are optimized after analyzing the results of tests with 6 LVDT's (Series 2). The positions of the 6 diagonal LVDT's are shown in Fig. 5. The results of series 2 show that some main shear cracks are out of the measuring range of units L1 and R1. The positions of units L3 and R3 are too close to the middle and may not measure the beginning of the crack appearance which is about at 600-800 mm of the support. Consequently, for further tests, only 2 LVDT's (L2 and R2) are used. The crack widths are measured on one side of the beams.
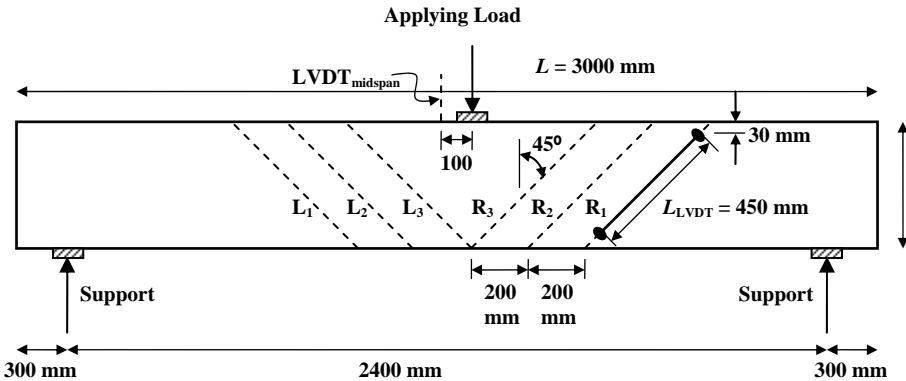

Fig. 5: Position of diagonal LVDT's (dashed-lines) and mid-span LVDT on the beams

2.4.   Displacements on the specimens

To measure the surface strains and monitor the crack width in detail a measuring mesh consisting of 241 elements, is placed on the surface of the beam (Fig. 6). A total number of 96 measuring points in 5 rows are installed at each node (Fig. 7). The distance between the measuring points is 100 mm and the position of the lowest row is 50 mm above the bottom of the beam which means that this row is exactly positioned at the height of the longitudinal reinforcing steel. In this way, obtaining the mean strain of the reinforcing bars would be easier. This measuring system is only applied on specimens from high strength concrete series (Series 6-10)
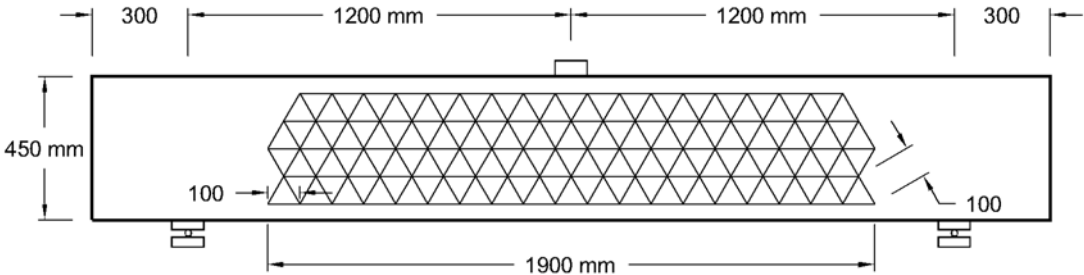

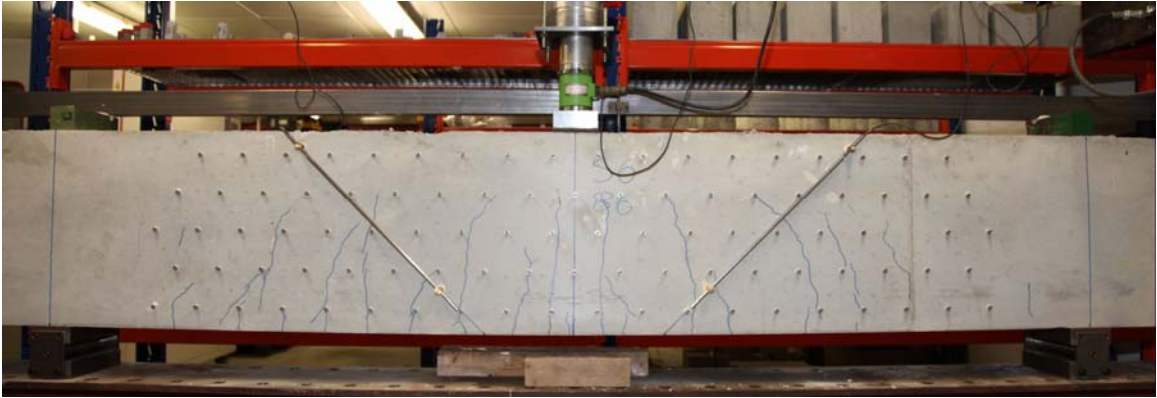**Fig. 6: The scheme of measuring mesh to monitor the displacements on the surface of the specimen**

Fig. 7: Measuring points installed on HSC beams to measure the strains and crack width on the beam

3. Testing procedure

The primary objective of the testing procedure is to investigate the time-dependency of shear behaviour of the beam and the shear crack growth in the unreinforced webs. The experiments involve determining the material properties, time dependency of flexural deformation, shear crack width and growth.

Table 3: The status of the casted beams (test dates and type of test)

Series	Label	Cast date	Test date	Type of Concrete	Type of test	Description
	S1B1	8 Oct 09	5 Nov 09	NSC	Short-term	Tested
	S1B2	8 Oct 09	5 Nov 09	NSC	Short-term	Tested
	S1B3	8 Oct 09	5 Nov 09	NSC	Short-term	Tested
Series 1	S1B4	8 Oct 09	5 Nov 09	NSC	Short-term	Tested
	S1B5	8 Oct 09	9 Nov 09	NSC	Short-term	Tested
	S1B6	8 Oct 09	9 Nov 09	NSC	Short-term	Tested
	S2B1	2 Nov 09	11 Jan 10	NSC	Short-term	Tested
	S2B2	2 Nov 09	12 Jan 10	NSC	Short-term	Tested
	S2B3	2 Nov 09	12 Jan 10	NSC	Short-term	Tested
Series 2	S2B4	2 Nov 09	13 Jan 10	NSC	Long-term	Tested
	S2B5	2 Nov 09	13 Jan 10	NSC	Long-term	Tested
	S2B6	2 Nov 09	13 Jan 10	NSC	Long-term	Tested
	S3B1	20 Nov 09	11 Feb 10	NSC	Short-term	Tested
	S3B2	20 Nov 09	11 Feb 10	NSC	Short-term	Tested
	S3B3	20 Nov 09	11 Feb 10	NSC	Short-term	Tested
Series 3	S3B4	20 Nov 09	15 Feb 10	NSC	Long-term	Failed
	S3B5	20 Nov 09	15 Feb 10	NSC	Long-term	In the setup
	S3B6	20 Nov 09	15 Feb 10	NSC	Long-term	Failed
	S4B1	2 Feb 10	8 Apr 10	NSC	Short-term	Tested
	S4B2	2 Feb 10	8 Apr 10	NSC	Short-term	Tested
	S4B3	2 Feb 10	8 Apr 10	NSC	Short-term	Tested
Series 4	S4B4	2 Feb 10	14 Apr 10	NSC	Long-term	In the setup
	S4B5	2 Feb 10	14 Apr 10	NSC	Long-term	In the setup
	S4B6	2 Feb 10	14 Apr 10	NSC	Long-term	Failed
	S5B1	7 Apr 10	–	NSC	Short-term	In store room
	S5B2	7 Apr 10	–	NSC	Short-term	In store room
	S5B3	7 Apr 10	–	NSC	Short-term	In store room
Series 5	S5B4	7 Apr 10	–	NSC	Long-term	In store room
	S5B5	7 Apr 10	–	NSC	Long-term	In store room
	S5B6	7 Apr 10	–	NSC	Long-term	In store room
	S6B1	17 Jun 10	14 Sep 10	HSC	Short-term	Tested
	S6B2	17 Jun 10	14 Sep 10	HSC	Short-term	Tested
	S6B3	17 Jun 10	14 Sep 10	HSC	Short-term	Tested
Series 6	S6B4	17 Jun 10	5 Oct 10	HSC	Long-term	In the setup
	S6B5	17 Jun 10	5 Oct 10	HSC	Long-term	Failed
	S6B6	17 Jun 10	5 Oct 10	HSC	Long-term	In the setup
	S7B1	10 Aug 10	–	HSC	Short-term	In store room
	S7B2	10 Aug 10	–	HSC	Short-term	In store room
	S7B3	10 Aug 10	–	HSC	Short-term	In store room
Series 7	S7B4	10 Aug 10	–	HSC	Long-term	In store room
	S7B5	10 Aug 10	–	HSC	Long-term	In store room
	S7B6	10 Aug 10	–	HSC	Long-term	In store room

The material parameters determined are cube compressive strength of concrete, splitting tensile strength of concrete and tensile strength of reinforcement. The dimension of the cubes used to determine the compressive and tensile strength is 150×150×150 mm. The ultimate

shear resistance of the concrete beams (3000×450×200 mm) is studied by a three-point bending test with short-term loading. Tests with sustained loading are also carried out in order to study time-dependent shear behaviour of the concrete beams.

The test setups are situated in a climate room with Relative Humidity of 50% and Temperature of 20°C to keep the environmental condition constant during the tests.

More details on short-term and long-term tests will be explained in the following sections.

3.1. Short-term loading

In order to obtain insight into the shear resistance of the beams, 3 short-term tests are carried out on each series of casting. The beams are loaded in 3-point-bending until failure. During loading, deflection and crack widths are measured by 3 LVDT's as shown in Fig. 5. The maximum load is reached within 15 minutes except for specimen S3B2 that took 28 minutes to fail. Since the load is applied by a hand-operated hydraulic jack, the rate of loading in each test varies between 0.3-2 kN/s.

The results of the short-term tests are a load-deflection curve, load-crack width curves and development of deflection and crack width in time. These results are used as reference results to obtain the mean value of the shear resistance of the beam. The crack pattern for each beam is also presented in chapter 5.

3.2. Long-term loading

The time-dependency of the shear resistance can be investigated by studying the effect of loading time on crack width and crack length; as the crack development may indicate a degrading process that results in a reduced shear capacity. However, unless the failure is reached, it is not possible to make a relationship between shear capacity and time. During loading, the width of the cracks is measured by means of two diagonal LVDT's and a manual LVDT.

A series of tests is carried out with different load levels ranging from 87% to 97% of the ultimate capacity (which is obtained from short-term tests). The corresponding time to reach failure (if it happens) will be used to find a relation between crack width, crack length and other material parameters like concrete strength.

Since the loading equipment (actuator and hydraulic jack) is hand-controlled, the oil pressure inside the actuator will decrease rapidly due to deflection of the beam and the accumulators can not cover the whole loss of the pressure. Hence, it is necessary to pump more oil to the setup to keep the force at the same level during the first couple of hours of test. Later on, the losses decrease and the accumulators are able to keep the pressure constant.

Monitoring of the cracks over longer periods of time is necessary in order to determine the overall rate of crack growth and to possibly relate this growth to failure of the beam. Besides the manual measurement system, the automatic equipment and software used have been undergoing continuous enhancements, and the system can now monitor the midspan deflection and diagonal strain and automatically record data while the beam is loaded. The

software is sensitive to both alteration of load and displacement, so any increase or decrease in input data will be recorded.

Monitoring of NSC beams involves diagonal strain of the beam at both sides and midspan deflection along with measuring the crack length after one hour, one day, one week, one month, three months and at the end of testing. Of course, if the load level changes, before and after applying the load, the cracks will be monitored.

4. Results of tensile and compressive strength of cubes

4.1.   Strength of cubes

Concrete strength increases with age as long as moisture and a favourable temperature are present for hydration of cement. To illustrate this, Fig. 8 contains the results of tests on concrete that is exposed to the air the entire time; its strength being 55% of the strength of moist-cured concrete at 28 days. Exposed to the air, 3 days after casting, the result is 80% and in air after 7 days, it is 90%. Quality curing and a sealing compound allow the concrete to continue in strength gain beyond 28 days as shown in Fig. 8 for moist-cured concrete.
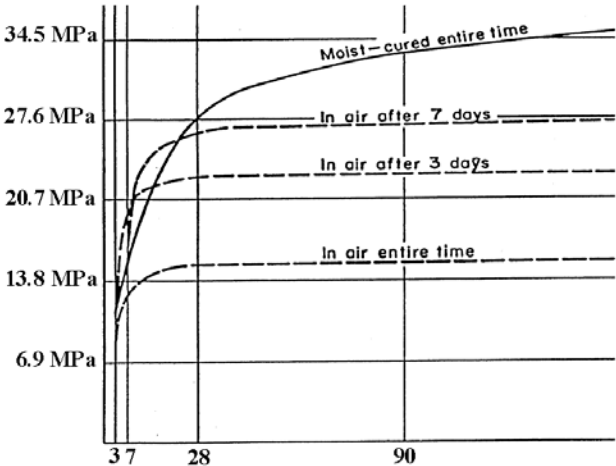

Fig. 8: Concrete strength with moisture present for curing, according to the Portland Cement Association [1]

After the concrete beams have been moved from the fog room (RH=99%, T=20°C) to the climate room (RH=50% and T=20°C) after 10-14 days, the strength of concrete increases because of further hydration. Hence, several compressive tests on cube samples are carried out on each series of casting to follow the strength development.

After performing the long-term test in cast 2 and 3, to obtain the actual strength of the concrete, cores are drilled with the axis normal to the surface of the beams. The cores are drilled in uncracked zone of the specimen (top-left or top-right of the beam). The diameter of the drilled cores is 100 mm and length is equal to the width of the beam (200 mm). Later on, they are cut into two pieces in the middle (2 × 100 mm). One core is drilled out of each beam; hence the total number of samples is 6. The results of the compressive tests on drilled cores are characterized by a large scatter, out of the range of compressive strength of the cubes. So the results of drilled cores are not taken into account. Besides, no more drilling is done for further tests.

Table 4. Compressive and tensile strength of cubes, series 1

No.	Dimensions [mm]	Age [days]	Store room* Fog/Climate	Loading rate [kN/s]	f_{cc} [MPa] Cubes	f_{cc} [MPa] Mean	f_{cspl} [MPa] Samples	f_{cspl} [MPa] Mean
1	150×150×150	4	F	13.5	15.27			
2	150×150×150	4	F	13.5	16.34	16.01		
3	150×150×150	4	F	13.5	16.41			
4	150×150×150	4	F	1.1			5.01	
5	150×150×150	4	F	1.1			2.97	4.01
6	150×150×150	4	F	1.1			4.06	
7	150×150×150	7	F	13.5	23.61			
8	150×150×150	7	F	13.5	24.13	23.66		
9	150×150×150	7	F	13.5	23.24			
10	150×150×150	7	F	1.1			3.44	
11	150×150×150	7	F	1.1			6.16	4.51
12	150×150×150	7	F	1.1			3.93	
13	150×150×150	14	F	13.5	28.70			
14	150×150×150	14	F	13.5	33.40	30.98		
15	150×150×150	14	F	13.5	30.81			
16	150×150×150	14	F	1.1			3.03	
17	150×150×150	14	F	1.1			3.19	3.09
18	150×150×150	14	F	1.1			3.04	
19	150×150×150	28	F	13.5	37.06			
20	150×150×150	28	F	13.5	38.95	38.18		
21	150×150×150	28	F	13.5	38.52			
22	150×150×150	28	F	1.1			3.50	
23	150×150×150	28	F	1.1			3.46	3.54
24	150×150×150	28	F	1.1			3.65	
25	150×150×150	57	C	13.5	32.72			
26	150×150×150	57	C	13.5	32.53	33.16		
27	150×150×150	57	C	13.5	34.22			
28	150×150×150	57	C	1.1			2.93	
29	150×150×150	57	C	1.1			2.67	2.76
30	150×150×150	57	C	1.1			2.67	
31	150×150×150	70	C	13.5	35.51			
32	150×150×150	70	C	13.5	30.70	35.50		
33	150×150×150	70	C	13.5	35.79			
34	150×150×150	70	C	1.1			2.90	
35	150×150×150	70	C	1.1			3.07	3.00
36	150×150×150	70	C	1.1			3.02	
37	150×150×150	103	C	13.5	40.59			
38	150×150×150	103	C	13.5	33.58	37.78		
39	150×150×150	103	C	13.5	39.16			
40	150×150×150	120	C	13.5	43.14			
41	150×150×150	120	C	13.5	35.71	37.67		
42	150×150×150	120	C	13.5	34.16			

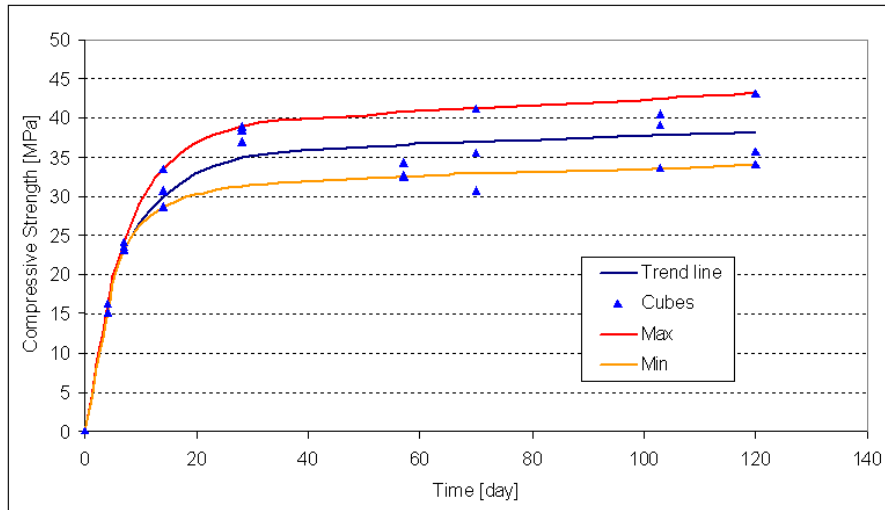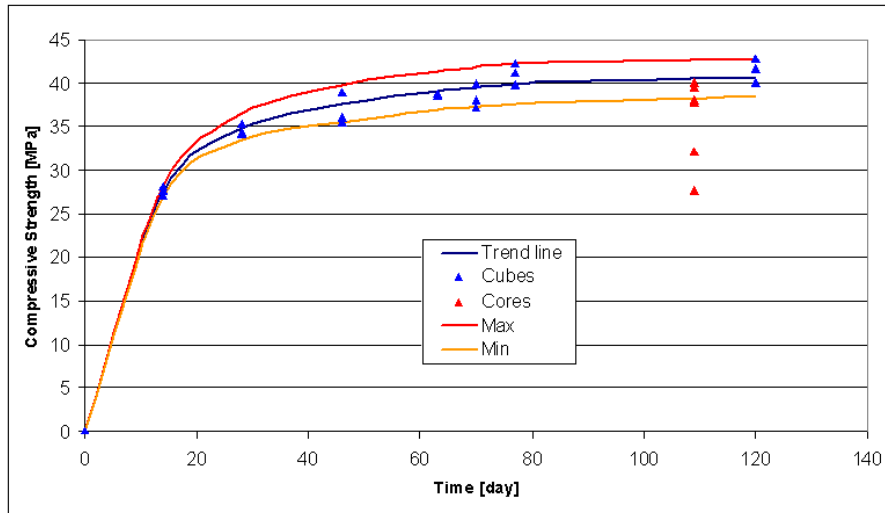* Cubes moved from the fog room (F) to the climate room (C) after 28 days

Fig. 9: Compressive strength of the cubes, Cast series 1

Table 5. Compressive and tensile strength of cubes and cores, series 2

No.	Dimensions [mm]	Age [days]	Store room* Fog/Climate	Loading rate [kN/s]	f_{cc} [MPa]		f_{cspl} [MPa]	
					Cubes	Mean	Cubes	Mean
1	150×150×150	14	F	13.5	27.72			
2	150×150×150	14	F	13.5	27.17	27.65		
3	150×150×150	14	F	13.5	28.12			
4	150×150×150	28	F	13.5	34.21			
5	150×150×150	28	F	13.5	34.33	34.62		
6	150×150×150	28	F	13.5	35.32			
7	150×150×150	46	F	13.5	35.41			
8	150×150×150	46	F	13.5	36.10	36.82		
9	150×150×150	46	F	13.5	38.95			
10	150×150×150	63	F	13.5	38.85			
11	150×150×150	63	F	13.5	38.72	38.81		
12	150×150×150	63	F	13.5	38.87			
13	150×150×150	70	F	13.5	37.19			
14	150×150×150	70	F	13.5	38.03	38.38		
15	150×150×150	70	F	13.5	39.92			
16	150×150×150	77	F	13.5	42.33			
17	150×150×150	77	F	13.5	41.24	41.12		
18	150×150×150	77	F	13.5	39.79			
19**	100×100	109	C	13.5	37.80			
20**	100×100	109	C	13.5	32.12			
21**	100×100	109	C	13.5	38.02	35.87		
22**	100×100	109	C	13.5	40.04			
23**	100×100	109	C	13.5	39.54			
24**	100×100	109	C	13.5	27.69			
25	150×150×150	120	F	13.5	41.72			
26	150×150×150	120	F	13.5	42.78	41.54		
27	150×150×150	120	F	13.5	40.12			

* All of the cubes stored in the fog room
** Drilled cores out of beams

16

Fig. 10: Compressive strength of the cubes, Cast series 2

Table 6. Compressive and tensile strength of cubes and cores, series 3

No.	Dimensions [mm]	Age [days]	Store room* Fog/Climate	Loading rate [kN/s]	f_{cc} [MPa]		f_{cspl} [MPa]	
					Cubes	Mean	Cubes	Mean
1	150×150×150	7	F	13.5	29.04		2.95	
2	150×150×150	7	F	13.5	25.97	28.37	2.87	2.93
3	150×150×150	7	F	13.5	30.09		2.96	
4	150×150×150	14	F	13.5	38.14		3.27	
5	150×150×150	14	F	13.5	37.33	38.80	3.29	3.30
6	150×150×150	14	F	13.5	40.92		3.35	
7	150×150×150	21	C	13.5	44.45		3.89	
8	150×150×150	21	C	13.5	45.84	45.93	3.80	3.85
9	150×150×150	21	C	13.5	47.50		3.85	
10	150×150×150	28	C	13.5	49.84		3.93	
11	150×150×150	28	C	13.5	42.57		3.72	
12	150×150×150	28	C	13.5	48.65	48.43	3.88	3.83
13	150×150×150	28	F	13.5	51.64		-	
14	150×150×150	28	F	13.5	47.00		-	
15	150×150×150	28	F	13.5	50.89		-	
16	150×150×150	49	F	13.5	48.22		4.19	
17	150×150×150	49	F	13.5	53.69	51.29	4.03	4.04
18	150×150×150	49	F	13.5	51.96		3.90	
19	150×150×150	63	C	13.5	51.04		4.30	
20	150×150×150	63	C	13.5	51.00	52.01	4.17	4.22
21	150×150×150	63	C	13.5	53.98		4.20	
22	150×150×150	70	C	13.5	48.03		-	
23	150×150×150	70	C	13.5	51.76	50.82	-	-
24	150×150×150	70	C	13.5	52.68		-	
25	150×150×150	84	C	13.5	49.01		4.03	
26	150×150×150	84	C	13.5	51.37	50.09	4.18	4.11
27	150×150×150	84	C	13.5	49.89		4.11	
28**	100×100	91	C	13.5	45.06		-	
29**	100×100	91	C	13.5	29.74		-	
30**	100×100	91	C	13.5	40.71	38.11	-	-
31**	100×100	91	C	13.5	31.14		-	
32**	100×100	91	C	13.5	35.66		-	
33**	100×100	91	C	13.5	46.32		-	
34	150×150×150	98	C	13.5	52.98		4.37	
35	150×150×150	98	C	13.5	54.79	53.45	4.68	4.50
36	150×150×150	98	C	13.5	52.57		4.45	
37	150×150×150	112	C	13.5	54.95	52.24	4.1	4.28

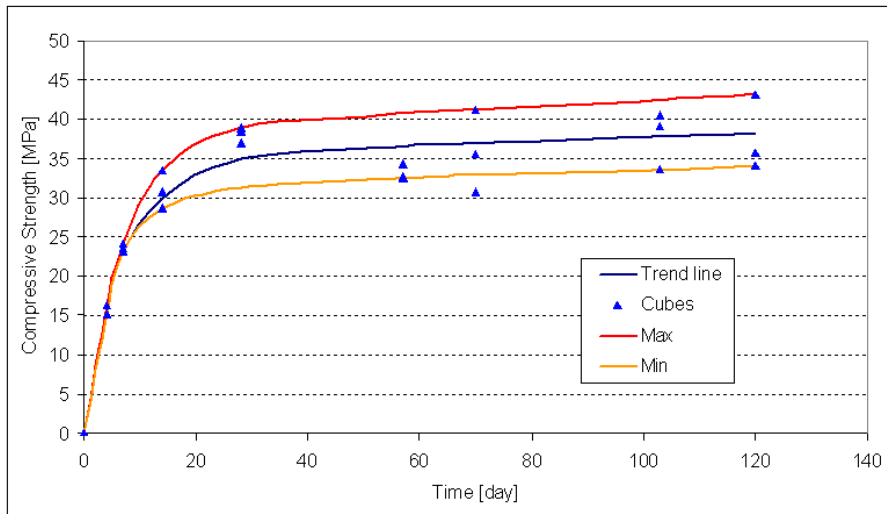| 36 | 150×150×150 | 112 | C | 13.5 | 48.34 | 4.5 |
| 39 | 150×150×150 | 112 | C | 13.5 | 53.42 | 4.23 |

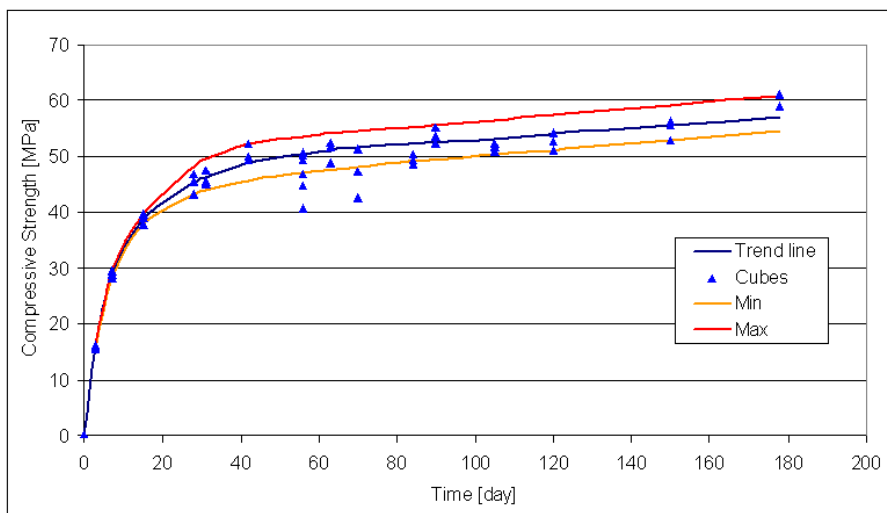**Fig. 11: Compressive strength of cubes (Cast 3)**

Fig. 12: Compressive strength of cubes (Cast 4)
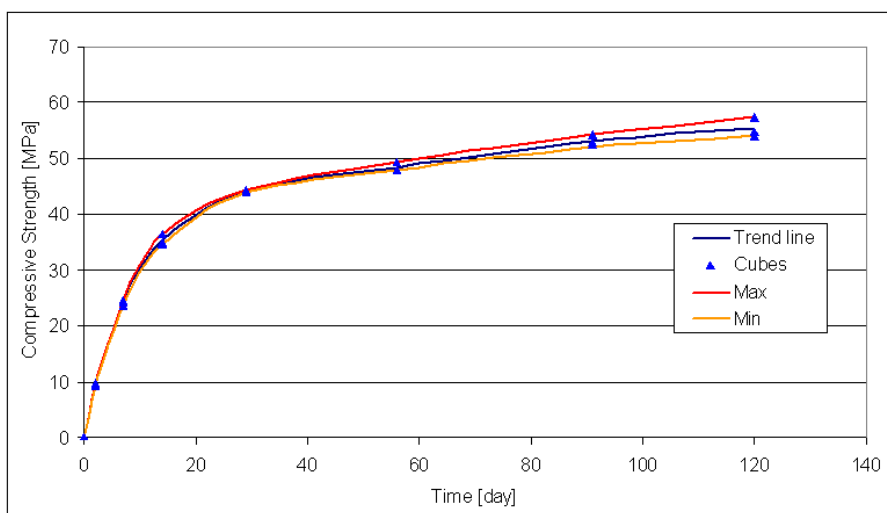

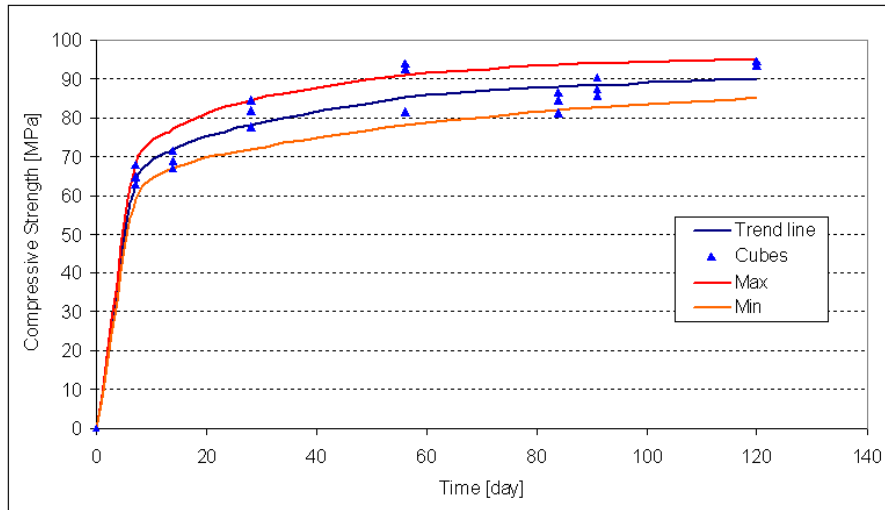**Fig. 13: Compressive strength of cubes (Cast 5)**

Fig. 14: Compressive strength of cubes (Cast 6)

4.2. Adjustment of shear capacity due to ageing of concrete

Based on the compressive strength of the concrete described in section 4.1, the shear resistance of the beams is recalculated using Rafla's formula (Appendix I) and ATENA software, see Table 7 to Table 12.

Table 7. Actual shear capacity of the beam based on compressive strength of the cubes, Series 1

Age [days]	f_{cc} [MPa] from curve (Blue line)	Shear Resistance Based on Rafla's formula [N]	Shear Resistance based on FEM in ATENA [N]
28	35	87334	81100
57	36.5	88941	81500
70	36.8	89551	82150
120	38.1	91119	81750

Table 8. Actual shear capacity of the beam based on compressive strength of the cubes, Series 2

Age [days]	f_{cc} [MPa] from curve (Blue line)	Shear Resistance based on Rafla's formula [N]	Shear Resistance based on FEM in ATENA [N]
28	34.8	87084	83050
46	37.6	90520	88050
77	40.0	93364	88750
120	40.7	94177	86750
147	40.8	94293	88500

Table 9. Actual shear capacity of the beam based on compressive strength of the cubes, Series 3

Age [days]	f_{cc} [MPa] from curve (Blue line)	Shear Resistance Based on Rafla's formula [N]	Shear Resistance based on FEM in ATENA [N]
28	47.7	101955	96100
49	50.5	104904	-
70	51.7	106144	-
112	52.3	106758	-
154	52.6	107063	-
365	53.4	107874	-

19

Table 10. Actual shear capacity of the beam based on compressive strength of the cubes, Series 4

Age [days]	f_{cc} [MPa] from curve (Blue line)	Shear Resistance Based on Rafla's formula [N]	Shear Resistance based on FEM in ATENA [N]
28	42.5	96237	-
56	50.5	104904	-
70	51.5	105938	-
120	54.0	108479	-
141	55.0	109478	-
180	57.0	111451	-

Table 11. Actual shear capacity of the beam based on compressive strength of the cubes, Series 5

Age [days]	f_{cc} [MPa] from curve (Blue line)	Shear Resistance Based on Rafla's formula [N]	Shear Resistance based on FEM in ATENA [N]
28	44.1	98032	-
56	48.4	102700	97100
90	53.2	107672	-
120	55.3	109777	-

Table 12. Actual shear capacity of the beam based on compressive strength of the cubes, Series 6

Age [days]	f_{cc} [MPa] from curve (Blue line)	Shear Resistance based on FEM in ATENA [N]
28	78	246800
56	85	258100
84	88	258100
120	90	260100

When using "3D Nonlinear Cementitious 2" element for concrete material, the tensile strength and fracture energy is calculated by the software based on the given compressive strength. In this element type, the fracture is modelled by an orthotropic smeared crack model based on Rankine tensile criterion and hardening–softening plasticity model based on the Men´etrey-William three-parameter failure surface is used to model concrete crushing (Men´etrey & William 1995), see Appendix III. Therefore the crack pattern changes if the strength changes.

Obviously there is some scatter in the results of ATENA. For instance in Table 7, when the compressive strength of the concrete increases from 36.8 MPa to 38.1 MPa, the shear capacity decreases but still in the range, even though the meshing and other parameters in the model are the same. The value of shear resistance is obtained at the end of each iteration step. Hence, this value depends on the step multiplier. Smaller step multiplier results more accurate shear resistance.

5. Results of short-term loading tests

5.1. Failure load and failure type

In all of the beams, shear cracks are observed at both the right and the left side of the specimen. In most of the cases, the crack formation is asymmetric and one crack propagates faster than the crack in the other side. Upon the growth of the crack to compression zone, the failure of concrete in that zone leads to a brittle explosive failure of the beam. The crack surface divides the beam into two pieces. That is the moment the load drops down suddenly and the specimen has failed. The failure load was considered to be the value at the highest peak (Fig. 15). In Table 13 the failure load of the beams tested in short-term loading is presented.

Table 13. The failure load of the specimen tested in short-term loading

Series	Cast date	Label	Age at loading [days]	Time of loading [sec]	Failure load P_u [kN]	Mean [kN]	COV
1	8 Oct 2009	S1B1	28	226	192.0	184.7	4.2%
		S1B2	28	92	176.1		
		S1B3	28	194	195.0		
		S1B4	28	258	174.1		
		S1B5	32	176	188.0		
		S1B6	32	162	182.9		
2	2 Nov 2009	S2B1	71	201	181.8	188.8	2.6%
		S2B2	72	444	192.7		
		S2B3	72	191	192.1		
3	20 Nov 2009	S3B1	83	773	202.1	204.9	1.2%
		S3B2	83	1697	208.0		
		S3B3	83	393	204.6		
4	2 Feb 2010	S4B1	65	683	187.4	194.7	4.0%
		S4B2	65	199	191.2		
		S4B3	65	346	205.4		
5	7 Apr 2010	S5B1					
		S5B2	Not tested				
		S5B3					
6	17 Jun 2010	S6B1	89	212	250.3	250.1	2.2%
		S6B2	89	239	256.8		
		S6B3	89	194	243.1		
7	17 Aug 2010	S7B1					
		S7B2	Not tested				
		S7B3					
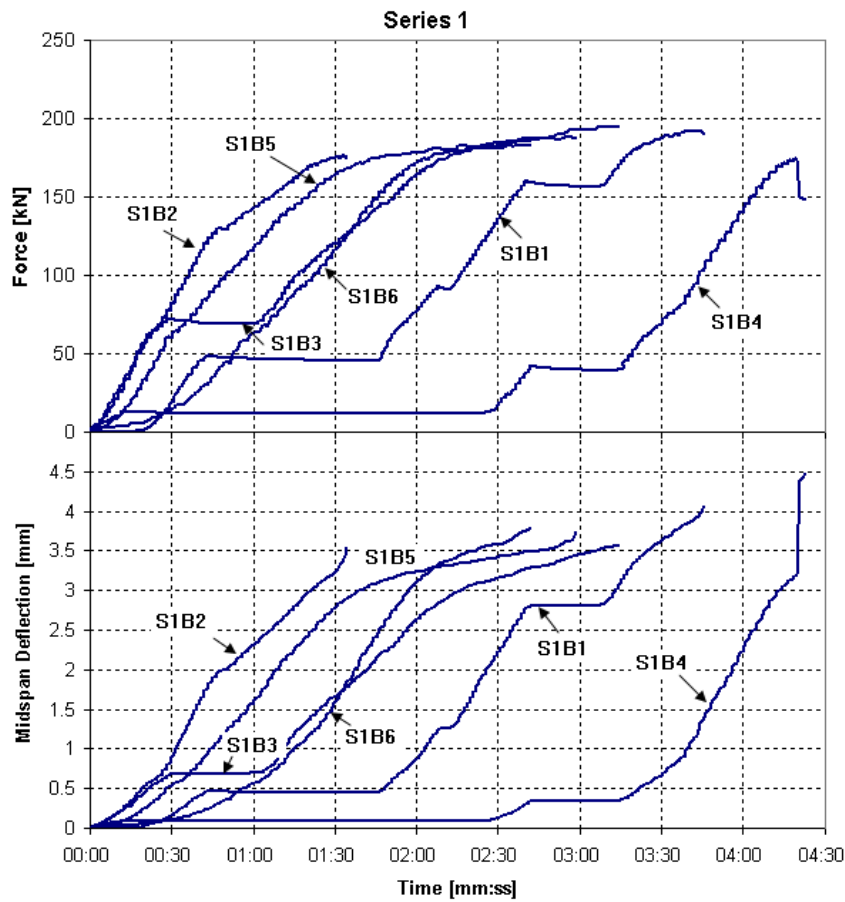
Fig. 15: Loading and midspan deflection of the beam in time, Series 1
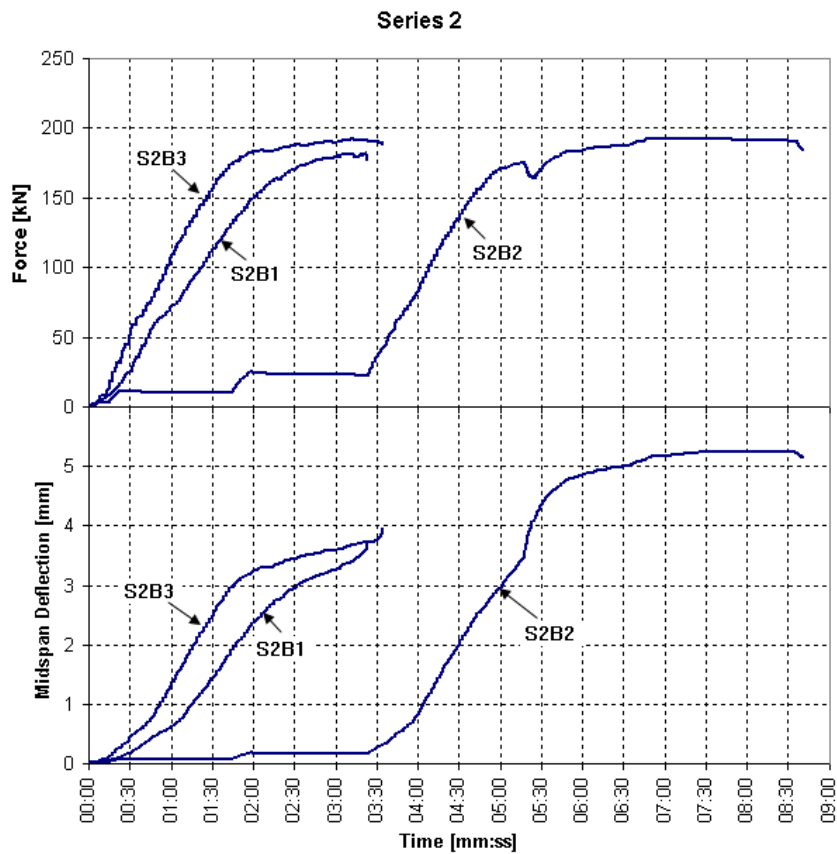
Fig. 16: Loading and midspan deflection of the beam in time, Series 2

22

The difference between the cracking pattern at failure for beams with Normal Strength Concrete and High Strength Concrete is illustrated in Fig. 17. The height of the compression zone in the HSC beams is smaller than in the NSC beams, whereas the angle at the base of the crack relative to the longitudinal axis is larger. The pattern of the shear cracks at the middle is inclined and the angle reduces, as at the tip the crack becomes almost parallel to the longitudinal axis. In Fig. 18, the surface of the crack for NSC and HSC can be seen. Obviously in HSC beams the shear crack was through the aggregates completely and not around them as is the case of NSC beams.
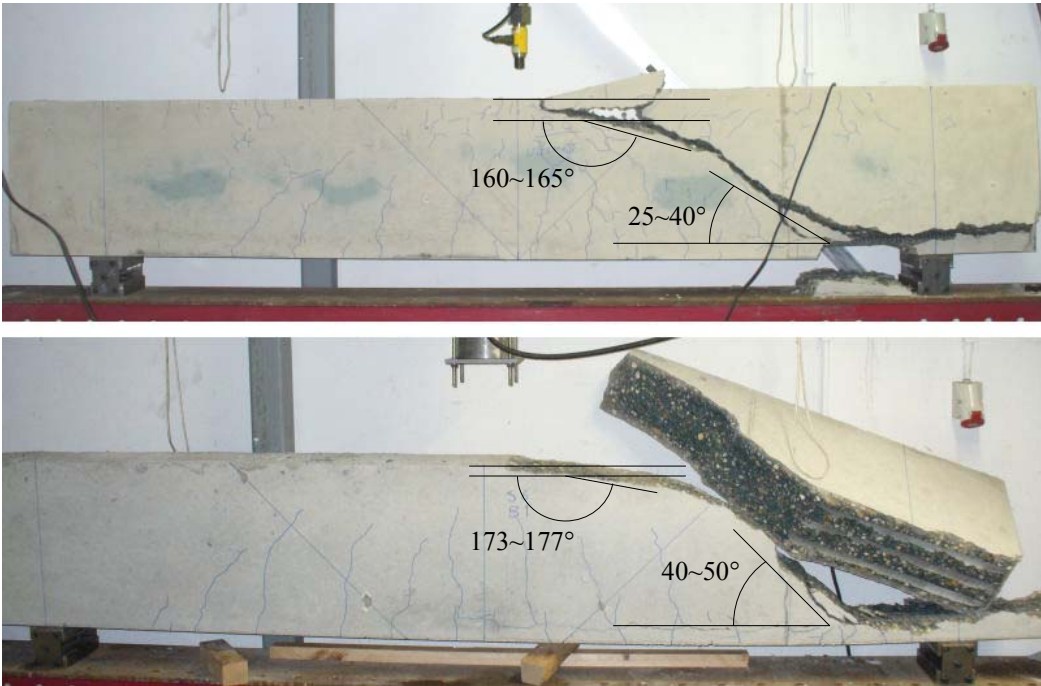
Fig. 17: Comparison of crack pattern in NSC (Top) and HSC beam (Bottom)

Fig. 18: Surface of crack in NSC (Left) and HSC beam (Right)

5.2. Deflection

Fig. 19 and Fig. 20 plots the load-deflection response for the beams tested in short-term loading. Deflections of the specimens were very similar in the same series.
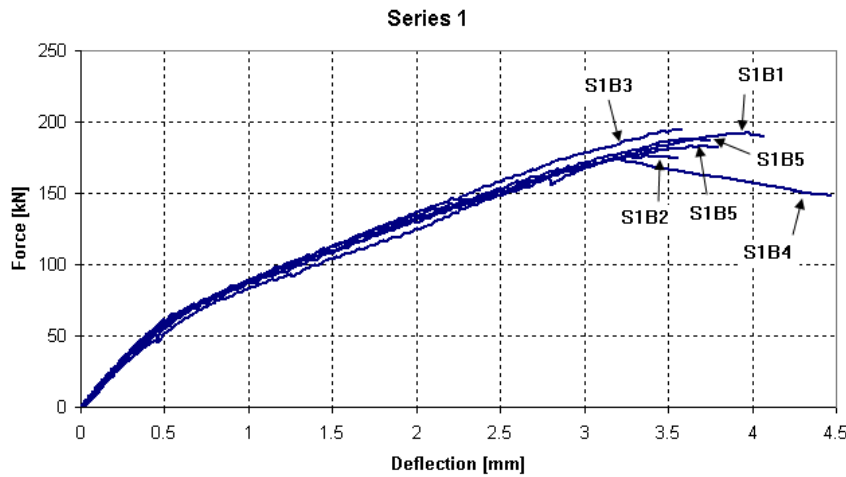
Fig. 19: Load-deflection curve, Specimens series 1

Fig. 20: Load-deflection curve, Specimens series 2. Numbers corresponds to the cracks in Fig. 28

5.3. Crack pattern

The crack patterns at failure for the Normal Strength Concrete (NSC) beams are shown in Fig. 21-Fig. 35. Similar figures present the crack pattern for HSC beams (Fig. 36-Fig. 38). The crack pattern shown in these figures are obtained after the failure of the beam. Hence, some of the bending cracks occur due to a large deformation of the beam after failure. There are three types of cracks shown in the figures; a Thick line represents the shear failure crack, semi-thick line represents clearly visible wide cracks which could cause the failure or contribute to the failure, and thin lines which are barely visible. It is tried to mark the shrinkage cracks before the test so these cracks are not drawn in crack pattern, but some thin cracks appeared during the test due to both shrinkage and loading stresses and it is hard to separate them from bending and shear cracks. Thus these cracks are also shown in the figures. Blue lines and green lines are representing the position of longitudinal reinforcement and the position of diagonal LVDT's, respectively.

It should be mentioned that in some specimens, the main shear crack is close to midspan and the crack tip goes under the loading plate (S2B2, S4B1 and S4B2). In this case, the failure is

24

not totally brittle but with a large deformation and crack opening, the load-carrying capacity decrease and slipping of the reinforcing bars leads to
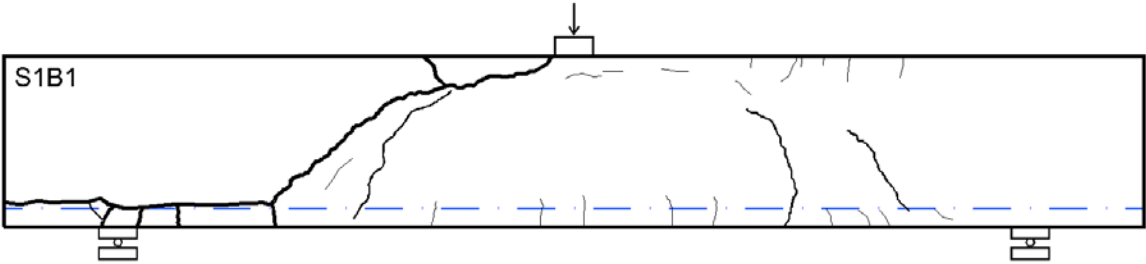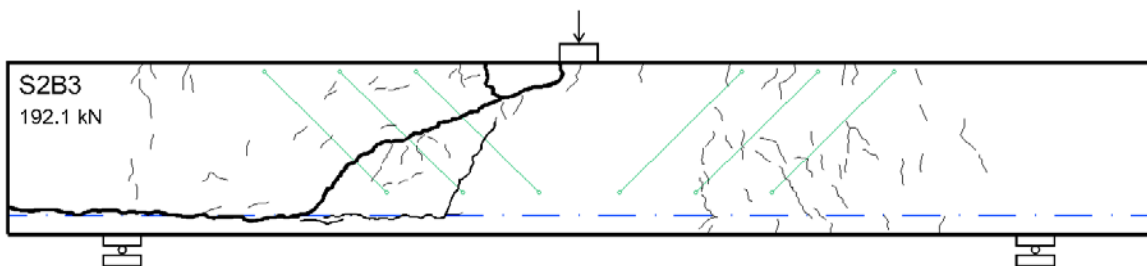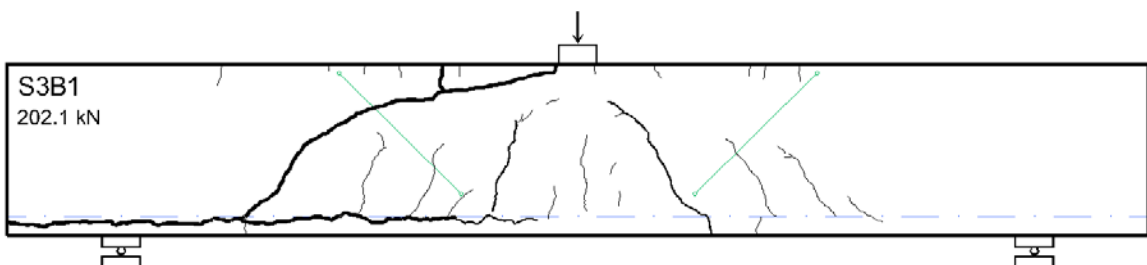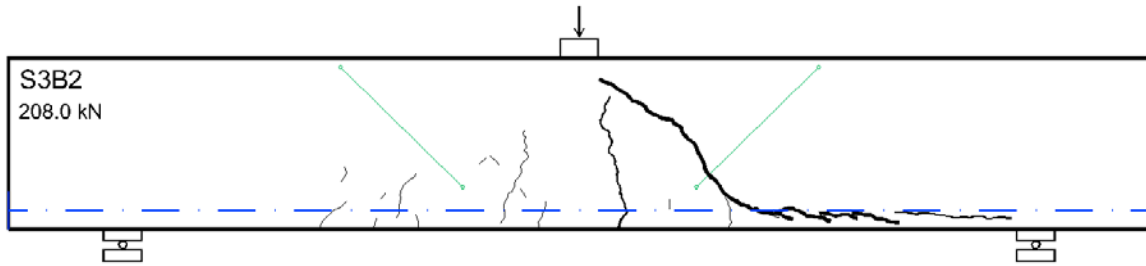

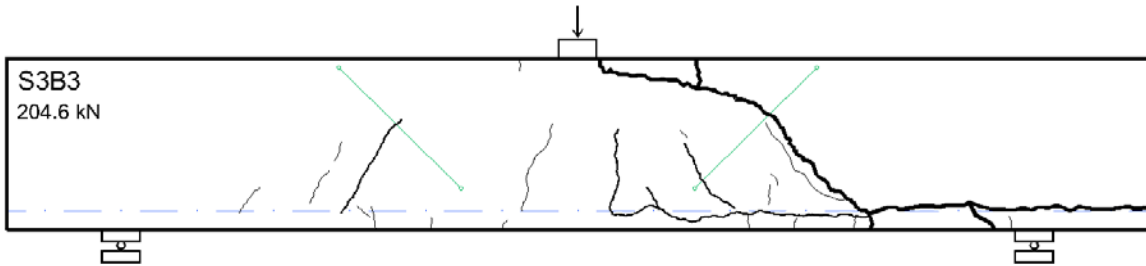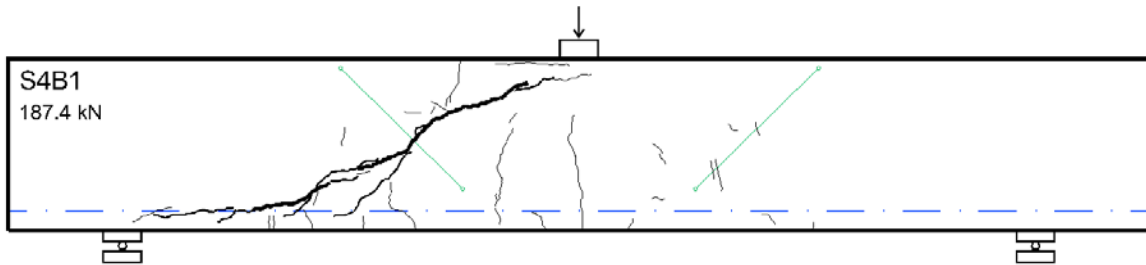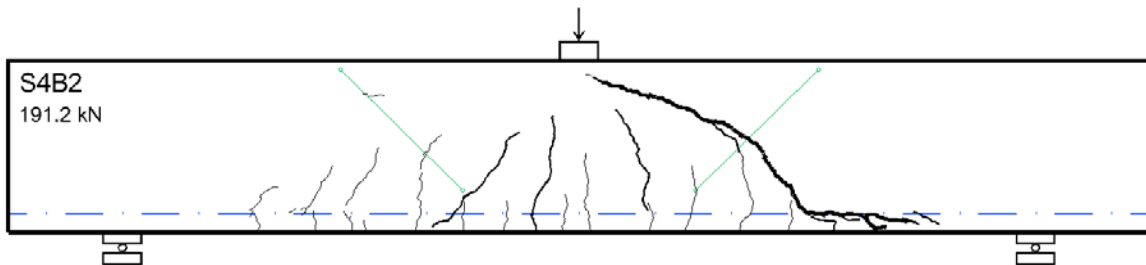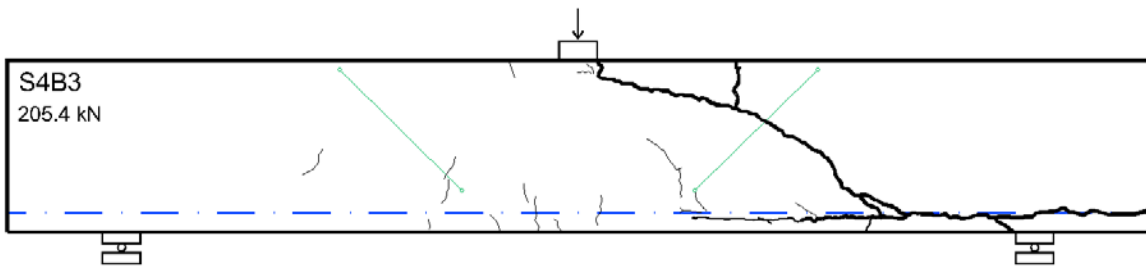**Fig. 21: Crack pattern in specimen S1B1**
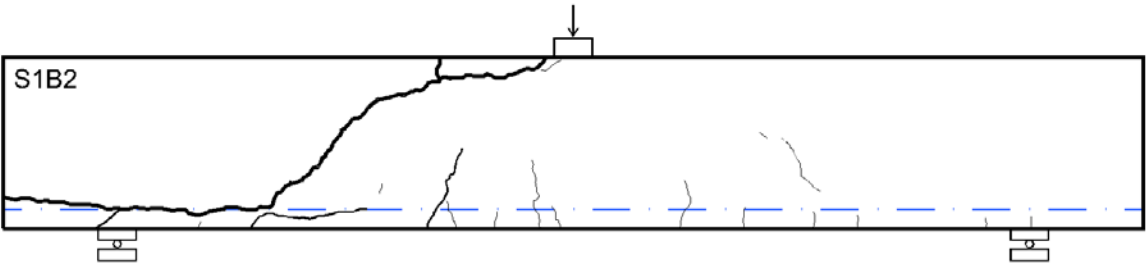
Fig. 22: Crack pattern in specimen S1B2
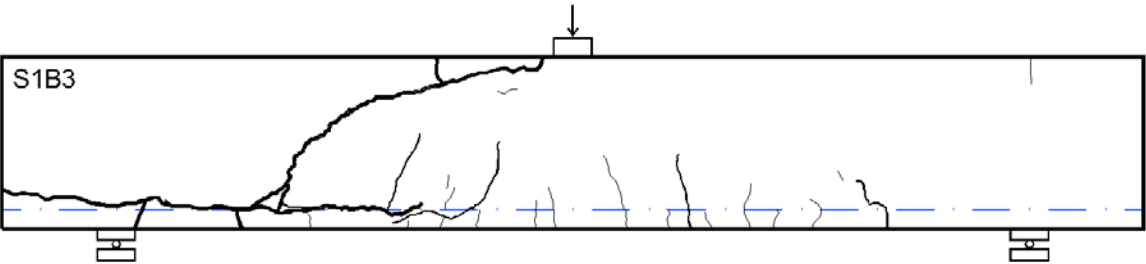
Fig. 23: Crack pattern in specimen S1B3
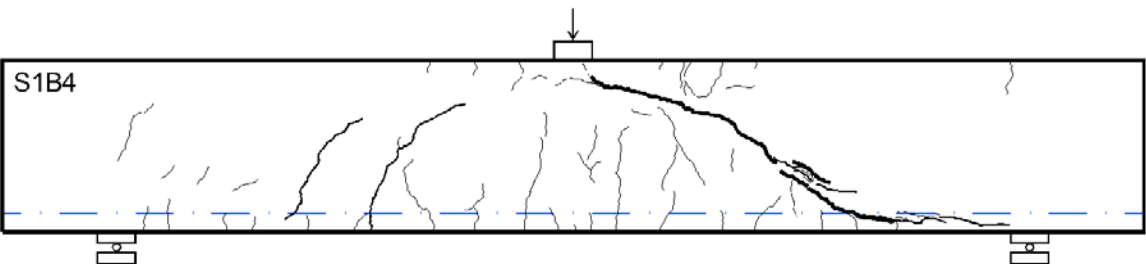
Fig. 24: Crack pattern in specimen S1B4
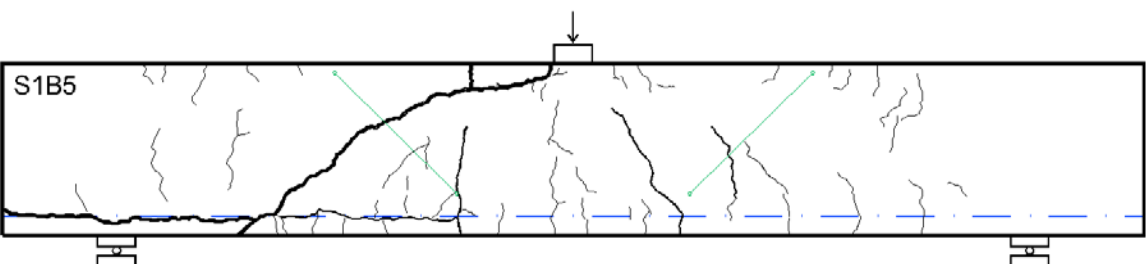
Fig. 25: Crack pattern in specimen S1B5
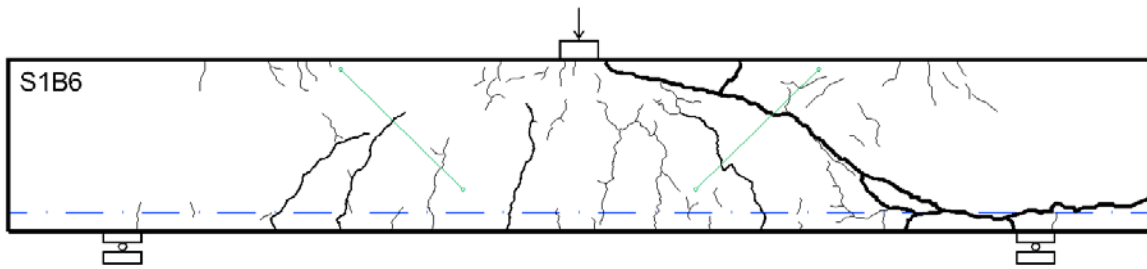
Fig. 26: Crack pattern in specimen S1B6
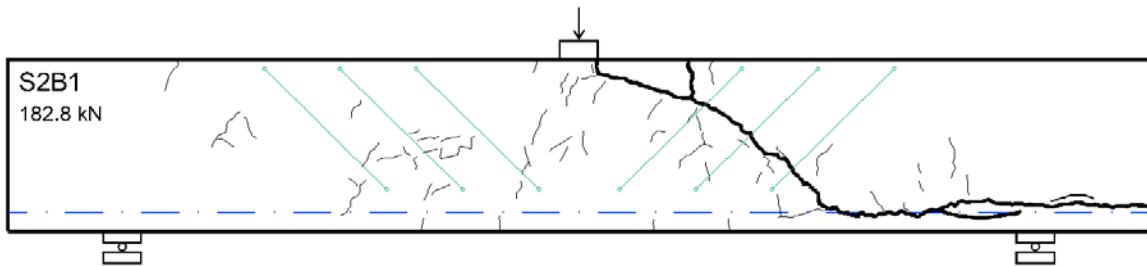
Fig. 27: Crack pattern in specimen S2B1
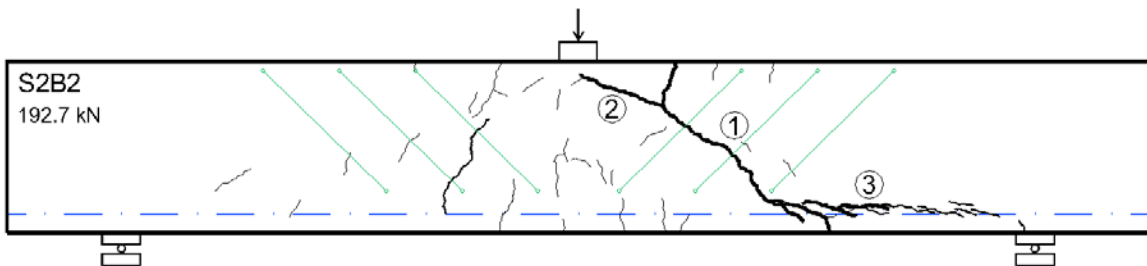
Fig. 28: Crack pattern in specimen S2B2

Fig. 29: Crack pattern in specimen S2B3

Fig. 30: Crack pattern in specimen S3B1

Fig. 31: Crack pattern in specimen S3B2

Fig. 32: Crack pattern in specimen S3B3

Fig. 33: Crack pattern in specimen S4B1

Fig. 34: Crack pattern in specimen S4B2

Fig. 35: Crack pattern in specimen S4B3
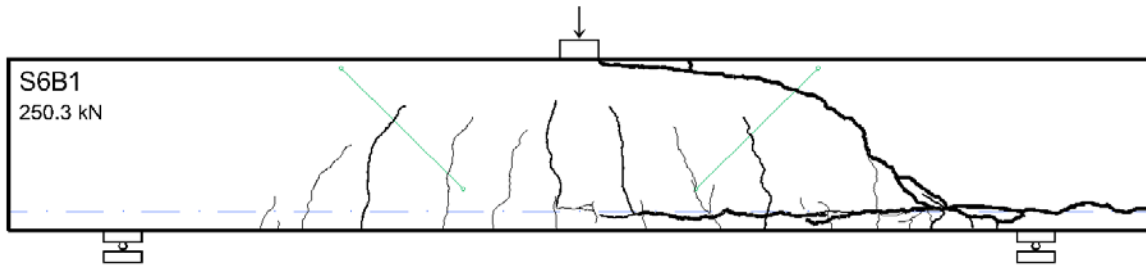
Fig. 36: Crack pattern in specimen S6B1
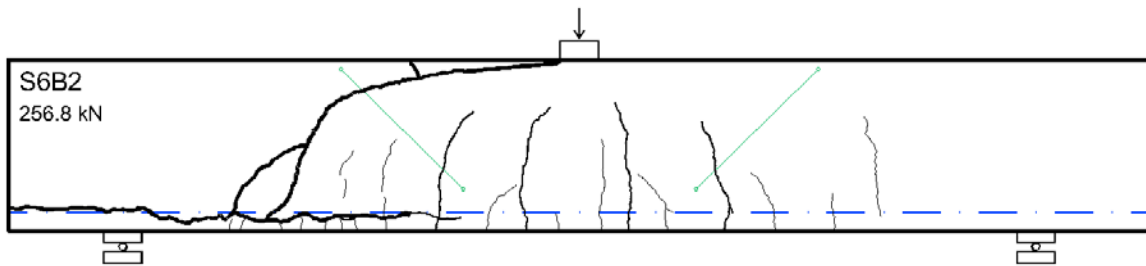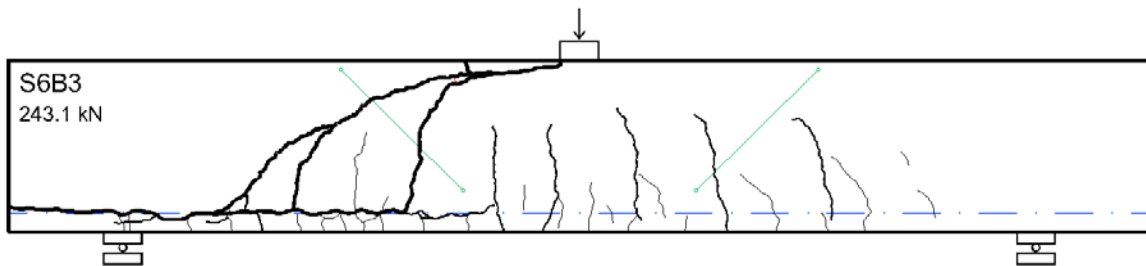

Fig. 37: Crack pattern in specimen S6B2

Fig. 38: Crack pattern in specimen S6B3

5.4. Summary of short-term loading tests

By short-term testing the three most important results obtained are:

- The failure load in each series which will be used as a reference value for the further tests in long-term loading. Moreover, the load-deflection curve could be helpful to predict the failure load of the beams subjected to long-term loading in early ages.
- The crack pattern and formation of the cracks to enble a comparison between the crack pattern (angle, inclination and length) in long-term loading and short-term loading.
- Formation of the crack, deflection of midspan and diagonal strain during loading. In some tests, e.g. specimen S2B2, the beam loaded up to the maximum capacity of the actuator and did not fail, but after a couple of minutes loading at this level, the shear failure occurred. This means that a beam subjected to a constant high load, could fail after short-term interval. The effect of creep, shrinkage and stress relaxation may be neglected in short-term loading.
- The scatter of the failure loads obtained by short-term loading is relatively small.

6. Results of long-term loading tests

As discussed earlier, the main goal of this research is to investigate the long-term loading of concrete beams without shear reinforcement. The specimens used to test in long-term loading have the same properties as the specimens tested in short-term loading. Three beams out of each series (except series 1 which are all tested in short-term loading) are tested in long-term loading.

One to three days after testing the beams in short-term loading, long-term loading test is started on the rest of the beams of the same series. It should be mentioned that because of the high level of loading which is close to the failure load (87-97% of the ultimate shear capacity) there is a probability that the beam will fail before the expected load is reached. In the upcoming sections, the level of loading and the results obtained within a couple of hours after loading will be discussed as well as actual long-term results.

6.1. Load level

6.1.1. Series 2

The first series which was tested in long-term loading is series 2. The long-term tests started at age of the concrete of 73 days (1 day after the short-term tests had been performed). In order to prevent failure of the beams during loading, the first series of long-term loading was carried out with a load level of 87% of the mean short-term ultimate capacity. The mean value of the failure load under short term testing was 188.8 kN which is considered to be the primary ultimate load. Thus the sustained load for the first step of loading was;

$$P_{sus,2} = 0.87\ P_{primary,2} = 0.87 \cdot 188.8 = 165\ \text{kN} \tag{1}$$

where $P_{primary,2}$ is the mean value of the short-term test results for series 2 and $P_{sus,2}$ is the sustained load applied to series 2.

The long-term load on the beams S2B4, S2B5 and S2B6 under 87% of the mean value of ultimate capacity was applied for 74 days. During this time, the strength of the concrete increased due to the further hydration. According to the results of shear resistance obtained with Rafla's formula from Table 8, the difference between the strength of the concrete of 77 days and 147 days of age is only 0.8 MPa, which leads to a 0.9% of increase in shear resistance.

$$P_{secondary,2} = 1.009\ P_{primary,2} = 1.009 \cdot 188.8 = 190.5\ \text{kN} \tag{2}$$

where, $P_{secondary,2}$ is the expected ultimate load for beam series 2 at concrete age 147 days.

After 74 days of sustained loading (Concrete age = 147 d), the load was increased step by step in order to determine the shear resistance. The loading steps with the duration of each step are shown in Table 14. Finally after 97 days testing under sustained load, the beams were loaded up to failure. The results were a little surprising. As shown in Table 14, the shear capacities of the beams are 6-8% higher than the expected value ($P_{primary,2}$).

Table 14. Load steps and duration of long-term loading, specimen series 2

Load step	S2B4	S2B5	S2B6
87% $P_{primary,2}$	165 kN 74 days	165 kN 74 days	165 kN 74 days
90% $P_{secondary,2}$	172 kN 4 days	172 kN 4 days	172 kN 4 days
92.5% $P_{secondary,2}$	176 kN 3 days	176 kN 3 days	176 kN 3 days
95% $P_{secondary,2}$	181.5 kN 6 days	181.5 kN 6 days	181.5 kN 6 days
97.5% $P_{secondary,2}$	186 kN 10 days	186 kN 10 days	186 kN 10 days
Failure	206.9 kN	202.4 kN	207.4 kN

6.1.2. Series 3

The long-term tests of series 3 started at a concrete age of 87 days (4 days after the short-term tests had been performed). This series of long-term loading is carried out at a load level of 95% of the ultimate capacity. The mean value of the failure load under short term tests was 205.1 kN which is considered to be the primary ultimate load. Thus the sustained load for the first step of sustained loading is;

$$P_{sus,3} = 0.95\ P_{primary,3} = 0.95 \cdot 205.1 = 195 \text{ kN} \tag{3}$$

where $P_{primary,3}$ is the mean value of the short-term test results for series 3 and $P_{sus,3}$ is the sustained load applied to series 3.

Specimen S3B3 failed during loading, at a load level of 194.8 kN. The long-term loading on beams S3B5 and S3B6 under 95% of the mean value of the ultimate capacity lasted 67 days. During this time the strength of the concrete increased because of further hydration. According to the results from Table 9, the difference between the strength of the concrete after 70 days and 154 days is 0.9 MPa, which leads to a 0.8% rise in shear resistance. After 1 year, the value of the compressive strength is predicted to be 53.4 MPa which is 1.7 MPa larger than the value after 70 days. Hence, based on Table 9 the shear resistance will theoretically increase with a factor 107874/106144=1.016.

$$P_{secondary,3} = 1.008\ P_{primary,3} = 1.006 \cdot 205.1 = 206.3 \text{ kN} \tag{4}$$
$$P_{tertiary,3} = 1.016\ P_{primary,3} = 1.016 \cdot 205.1 = 208.4 \text{ kN} \tag{5}$$

where, $P_{secondary,3}$ and $P_{tertiary,3}$ are the expected ultimate loads for beams of series 3 at a concrete age of 154 days and 365 days, respectively.

After 67 days of sustained loading (Concrete age = 154 d), the load was increased to 200 kN. The loading steps with the duration of each step are shown in Table 15. The load level of 200 kN was maintained for 70 days. Because the capacity of the setup was already reached (200 kN) the actuators and load cells were replaced by new ones, in order to apply higher loads up to 400 kN. Substituting of the new setup, took 55 days and during this time, all the specimens were unloaded.

After reloading the beams, specimen S3B6 failed at a load level of 196 kN. The last beam (S3B5) is still under long-term loading.

Table 15. Load steps and duration of long-term loading, specimen series 3

Load step	S3B4	S3B5	S3B6
95% $P_{\text{primary},3}$	Failed at 194.8 kN –	195 kN 67 days	195 kN 67 days
97% $P_{\text{secondary},3}$	– –	200 kN 70 days	200 kN 70 days
Unloaded	– –	– 55 days	– 55 days
97% $P_{\text{secondary},3}$	– –	200 kN Since 16 Aug 10	Failed at 196 kN –

6.1.3. Series 4

Long-term test on series 4 started at a concrete age of 71 days (6 days after the short-term tests had been performed). This series of long-term loading is also carried out at a load level of 95% of the ultimate capacity. Based on Table 13, the mean value of the failure load under short term tests is 194.7 kN which is considered to be the primary ultimate load. Thus the sustained load for the first step of loading is;

$$P_{\text{sus},4} = 0.95 \ P_{\text{primary},4} = 0.95 \cdot 194.7 = 185 \text{ kN} \tag{6}$$

where, $P_{\text{primary},4}$ is the mean value of short-term test results for series 4 and $P_{\text{sus},4}$ is the sustained load applied to series 4.

Specimen S4B6 failed 2.5 hours after applying the sustained load, at a load level of 185 kN. The long-term loading on beams S4B4 and S4B5 under 95% of the mean value of ultimate capacity lasted 70 days until the beams were unloaded for the installation of new equipment to increase the capacity.

According to the results of the shear resistance based on Rafla's formula from

Table 10, the difference between the strength of the concrete in 70 days and 141 days is 3.5 MPa, which theoretically would lead to an increase of the shear resistance with a factor 109478/105938=1.033. After 6 months, the value of the compressive strength was predicted to be 57 MPa which is 5.5 MPa higher than the value after 70 days. Hence, based on Table 9 the shear resistance would expected to be increased by a factor 111451/105938=1.052.

$$P_{secondary,4} = 1.038\ P_{primary,4} = 1.033 \cdot 194.7 = 201.1 \text{ kN} \tag{7}$$
$$P_{tertiary,4} = 1.052\ P_{primary,4} = 1.052 \cdot 194.7 = 204.8 \text{ kN} \tag{8}$$

where, $P_{secondary,4}$ and $P_{tertiary,4}$ are the expected ultimate loads for beam series 4 at a concrete age of 150 days and 180 days, respectively.

After 70 days of sustained loading (Concrete age = 141 d) and 55 days unloading time, the beams were reloaded to 190 kN. The loading steps with the duration of each step are shown in

Table 16. Beams S4B4 and S4B5 have been under 190 kN until present.

Table 16. Load steps and duration of long-term loading, specimen series 4

Load step	S3B4	S3B5	S3B6
95% $P_{primary,4}$	185 kN 70 days	185 kN 70 days	185 kN Failed after 2.5 hours
Unloaded	– 55 days	– 55 days	– –
95% $P_{secondary,4}$	190.5 kN Since 16 Aug 10	190.5 kN Since 16 Aug 10	– –

6.1.4. Series 6

Long-term test on series 6 started at a concrete age of 110 days (21 days after the short-term tests had been performed). The first series of long-term loading on high strength concrete is carried out with a load level at 90% of the ultimate shear capacity. Based on Table 13, the mean value of the failure load under short term loading was 250.1 kN which is considered to be the primary ultimate shear load. Thus the sustained load for the first step of loading is;

$$P_{sus,6} = 0.9\, P_{primary,6} = 0.9 \cdot 250.1 = 225.0 \text{ kN} \tag{9}$$

where, $P_{primary,6}$ is the mean value of the short-term shear capacity of series 6 and $P_{sus,6}$ is the sustained load applied to series 6.

Specimen S6B5 failed during loading at a load level of 221 kN. The long-term loading on beams S6B4 and S6B6 under 224 kN (90% of the mean value of ultimate capacity) was maintained out from October 5, 2010 until now.

6.2. Observations within a couple of hours after applying the sustained load

The most remarkable results are the results obtained in the first couple of hours when midspan deflection and crack width increase. There is of course a limit for crack width and maximum deflection; reaching the maximum deflection possibly takes a couple of months due to creep of the concrete but the maximum crack width could be reached within a couple of hours or a couple of days.

In the following figures, a time histories of load, midspan and diagonal strain are presented for each beam in the first 6 hours of loading. The irregularities on load-time curve are due to adjustments of the load at a certain level. The values of deflection and crack width for each curve after 6 hrs are shown above the curve and compared with the final value at the end of testing (highlighted value).
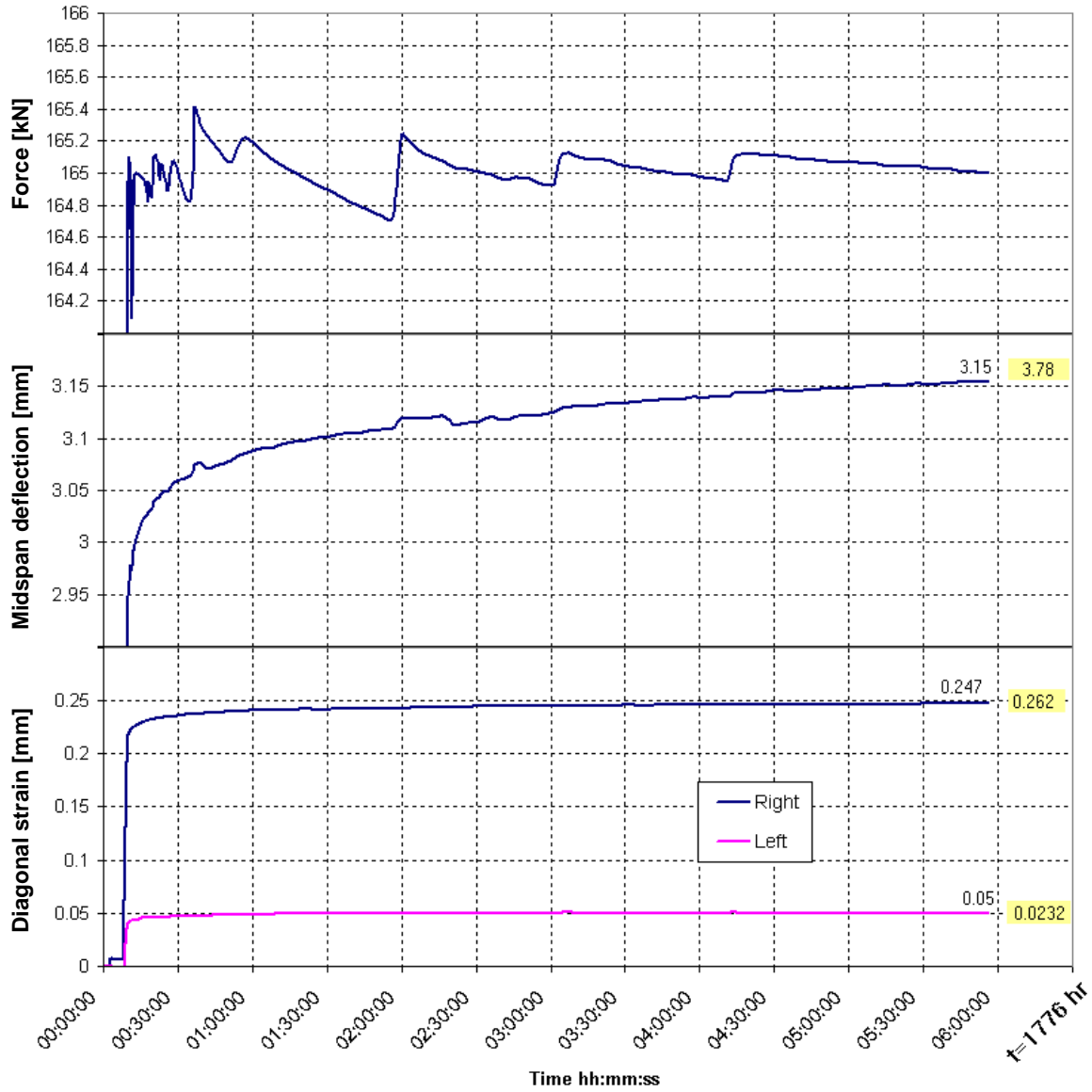
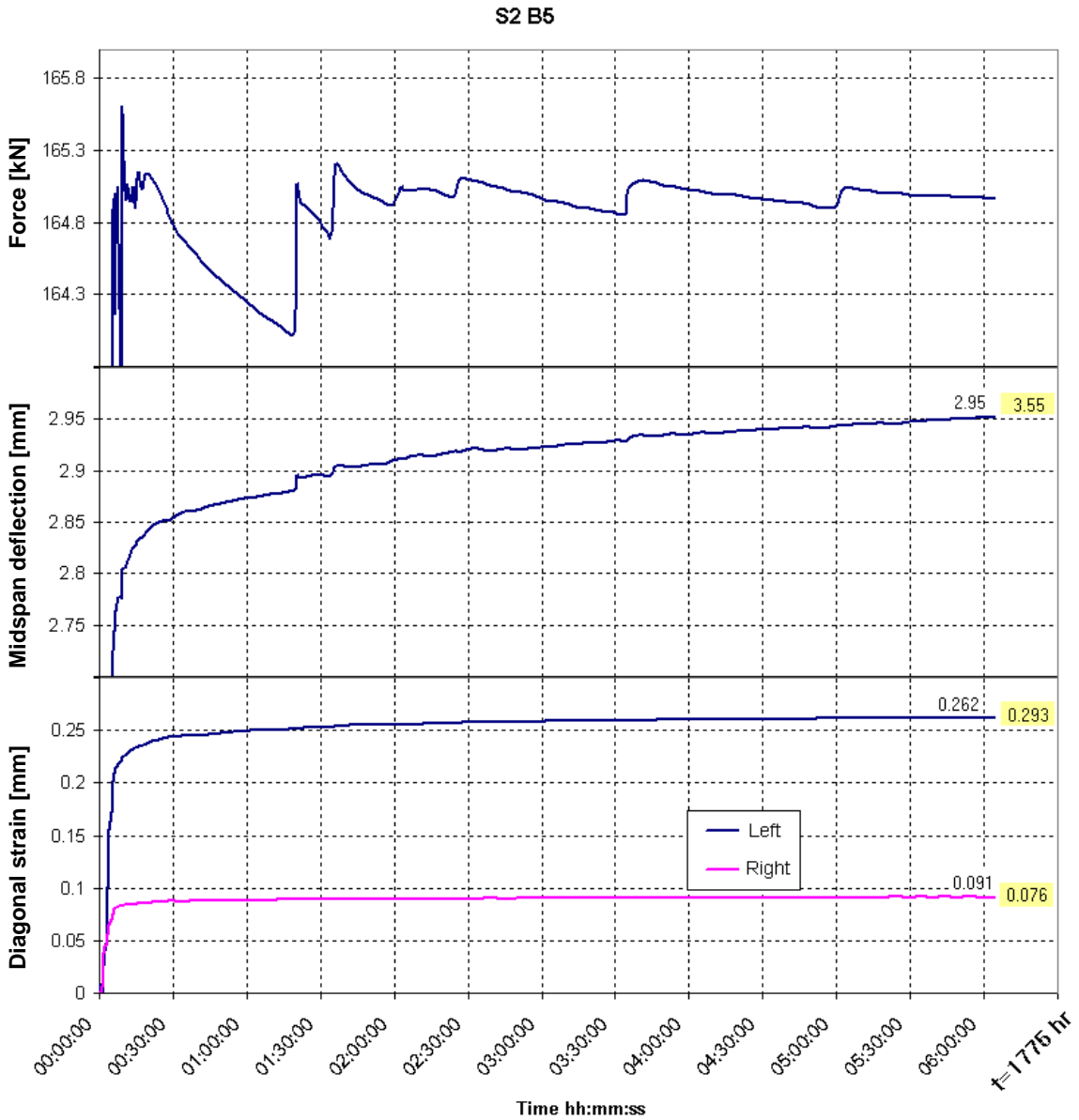**Fig. 39: Time-history of load, midspan and diagonal strain in the first 6 hours, Specimen S2B4**

Fig. 40: Time-history of load, midspan and diagonal strain in the first 6 hours, Specimen S2B5

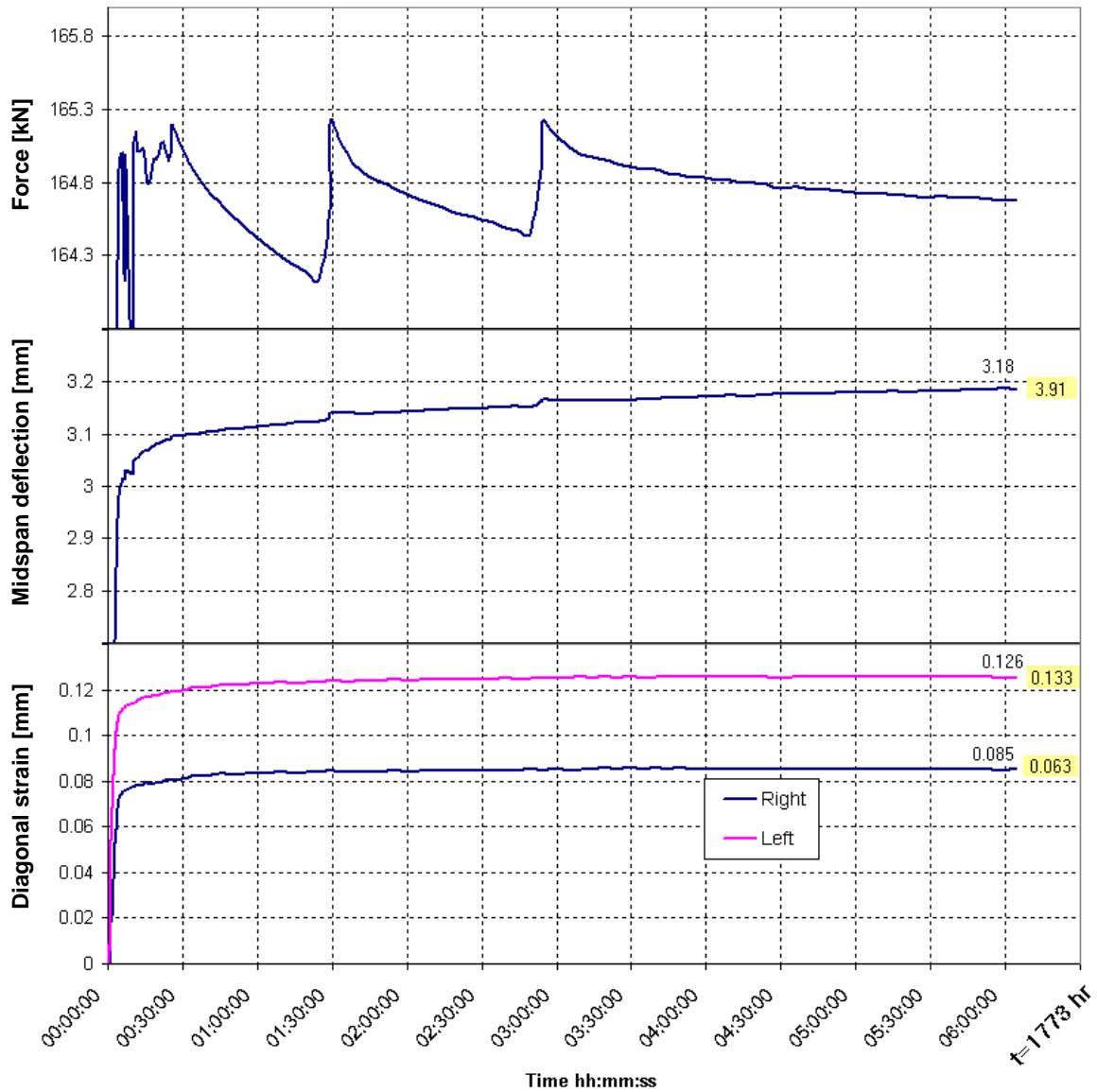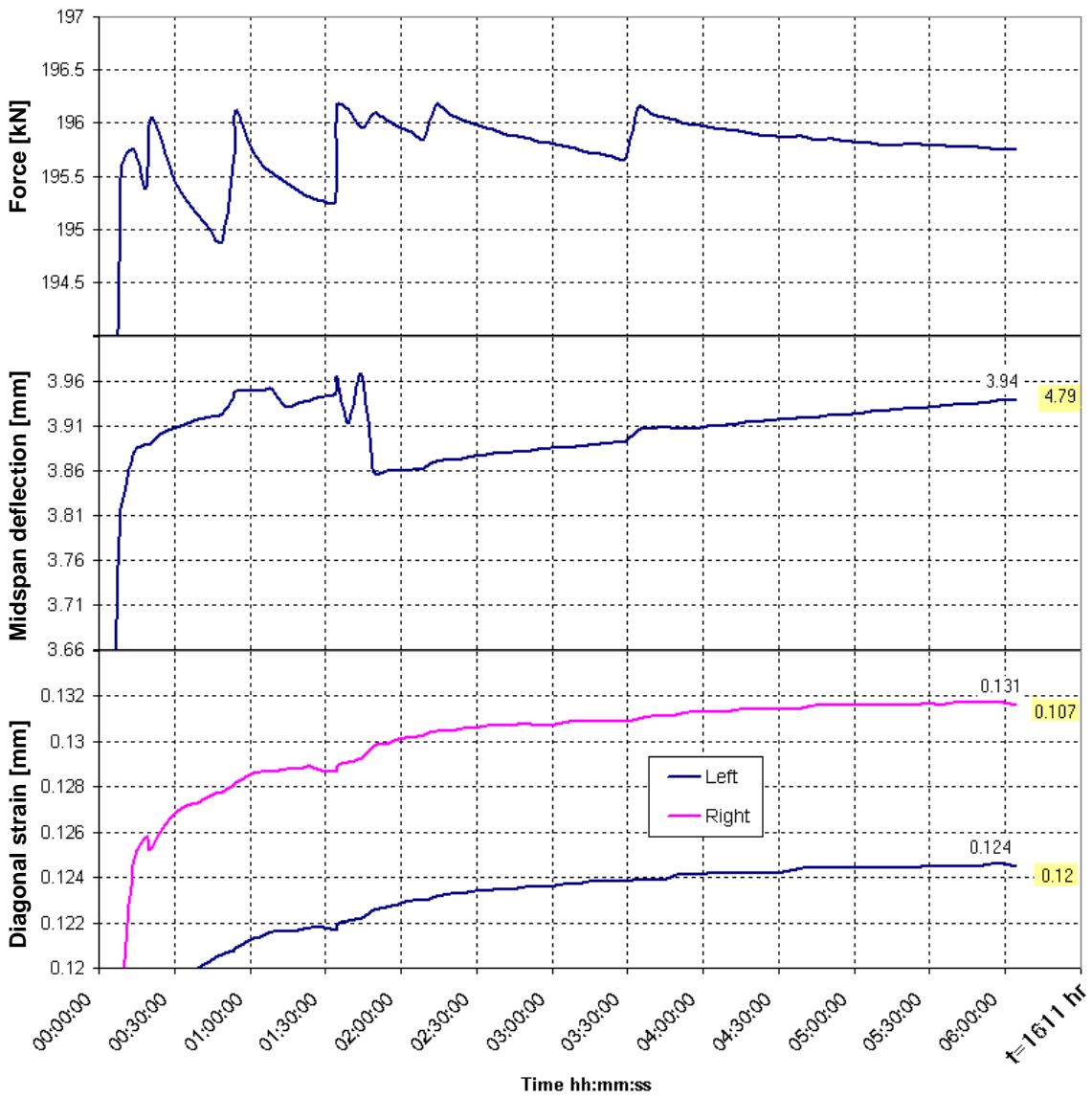**Fig. 41: Time-history of load, midspan and diagonal strain in the first 6 hours, Specimen S2B6**

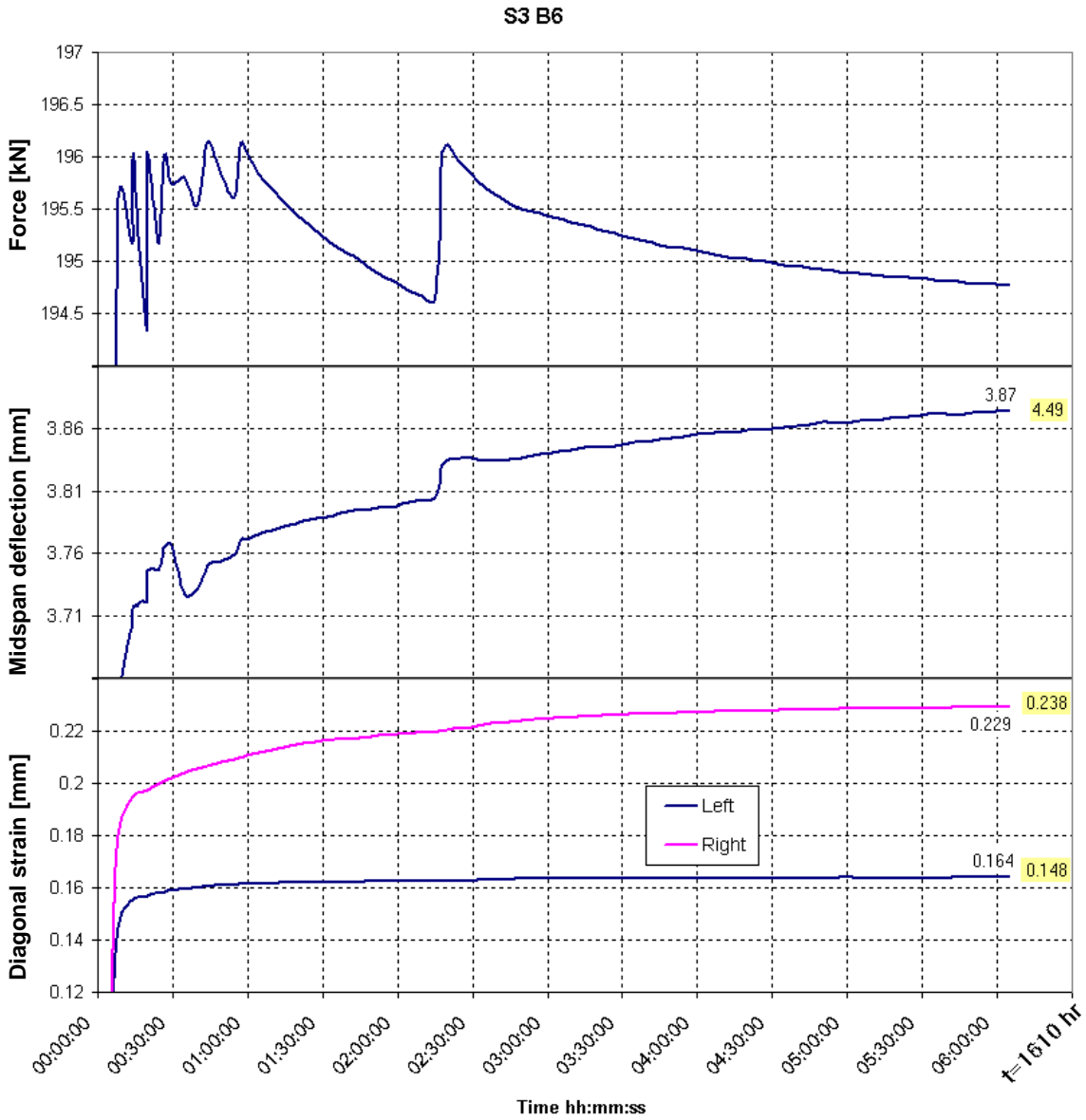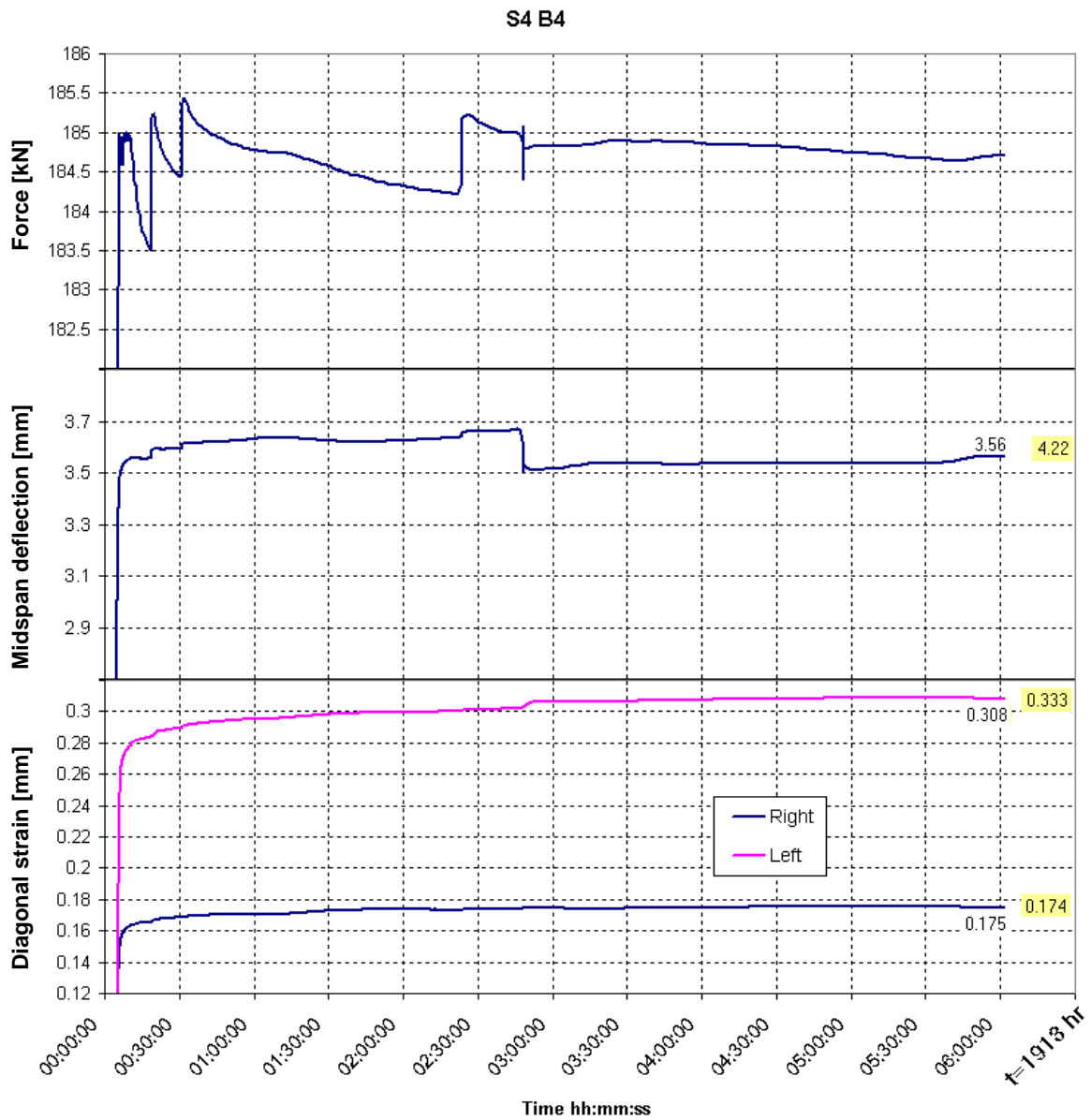**Fig. 42: Time-history of load, midspan and diagonal strain in the first 6 hours, Specimen S3B5**

Fig. 43: Time-history of load, midspan and diagonal strain in the first 6 hours, Specimen S3B6

Fig. 44: Time-history of load, midspan and diagonal strain in the first 6 hours, Specimen S4B4
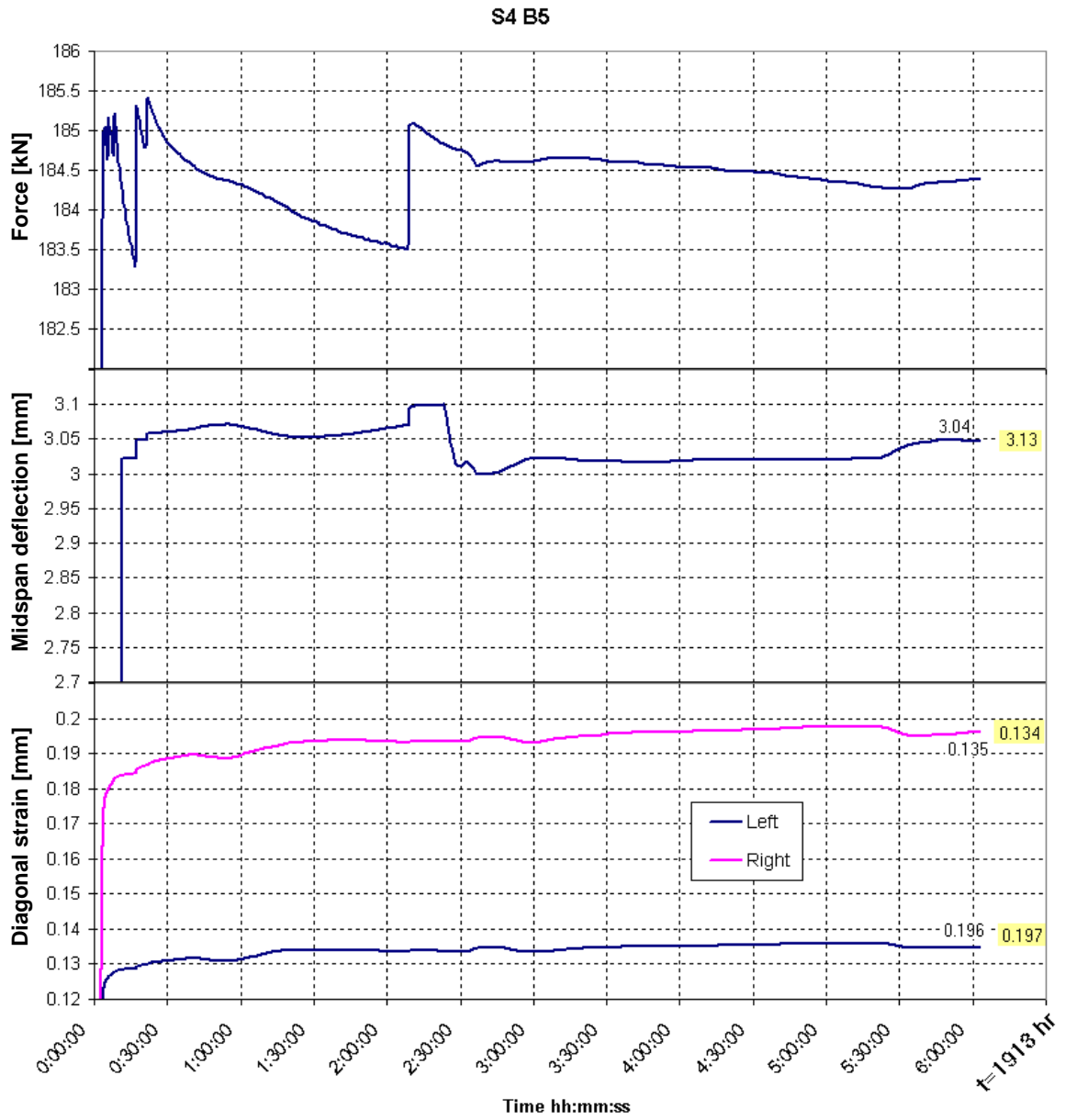
Fig. 45: Time-history of load, midspan and diagonal strain in the first 6 hours, Specimen S4B5
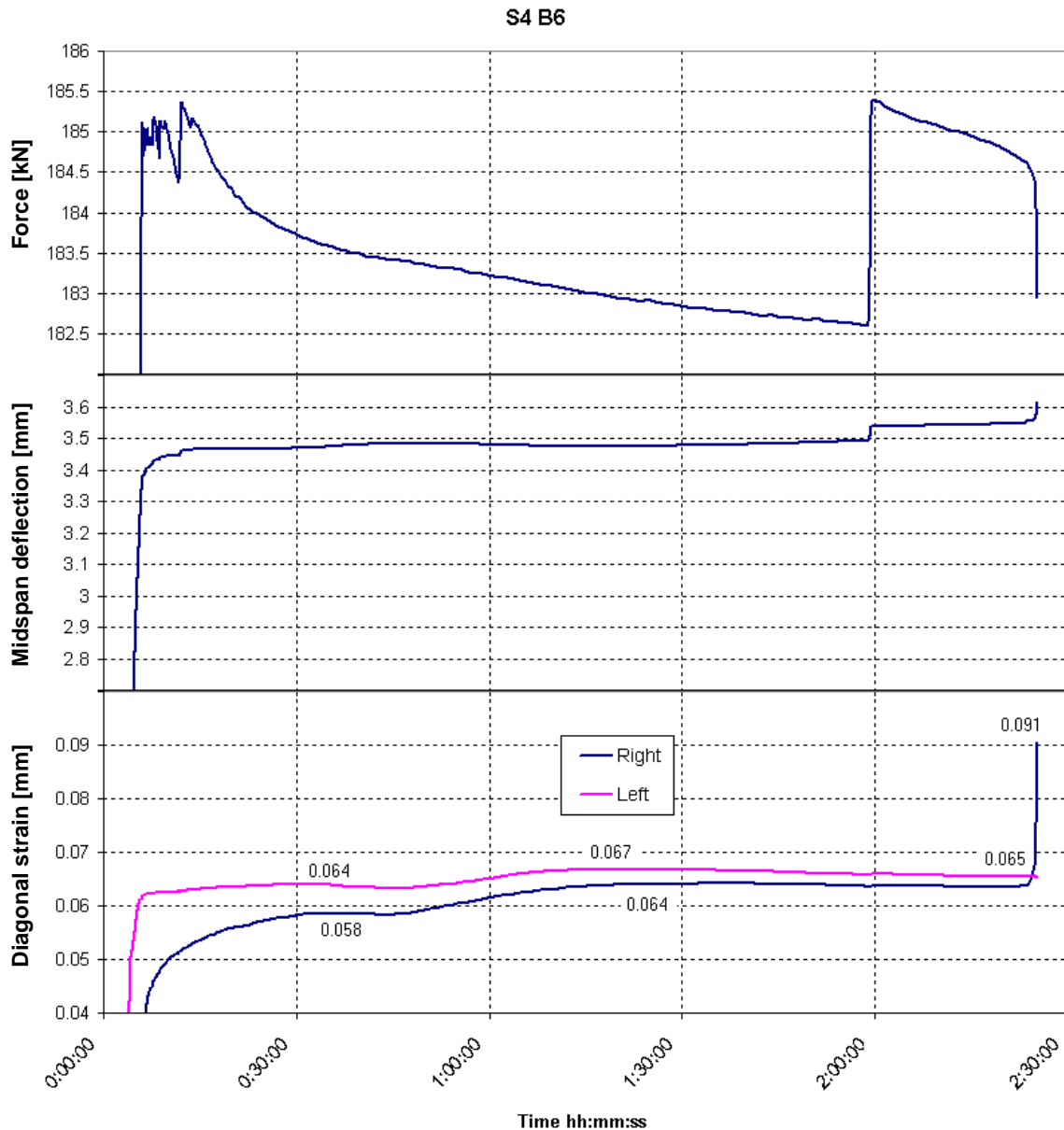
Fig. 46: Time-history of load, midspan and diagonal strain in the first 6 hours, Specimen S4B6

6.3. Long-term results

In this section the results obtained from long-term loading of the beams will be shown. These results consist of time history of the load measured by a load-cell, midspan deflection measuredb y a LVDT and diagonal strain of the beam measured by two LVDT's.

It is mentioned previously that the load was applied by a hand-controlled hydraulic jack and had to be adjusted as well. Any irregularities on the load-time curve are caused by adjustment of the applied load on the specimen.

The results are recorded every 15 minutes by the software, automatically. Moreover, since the software is sensitive to both alteration of load and displacement thus any increase or decrease in input data, is recorded. Currently, long-term loading of two beams (S2B4 and S2B5) are

finished and the rest of the beams are still under sustained loading as mentioned in Table 3.
the results of sustained loading on specimen S2B4 and S2B5 are shown in Fig. 47 and Fig. 48.
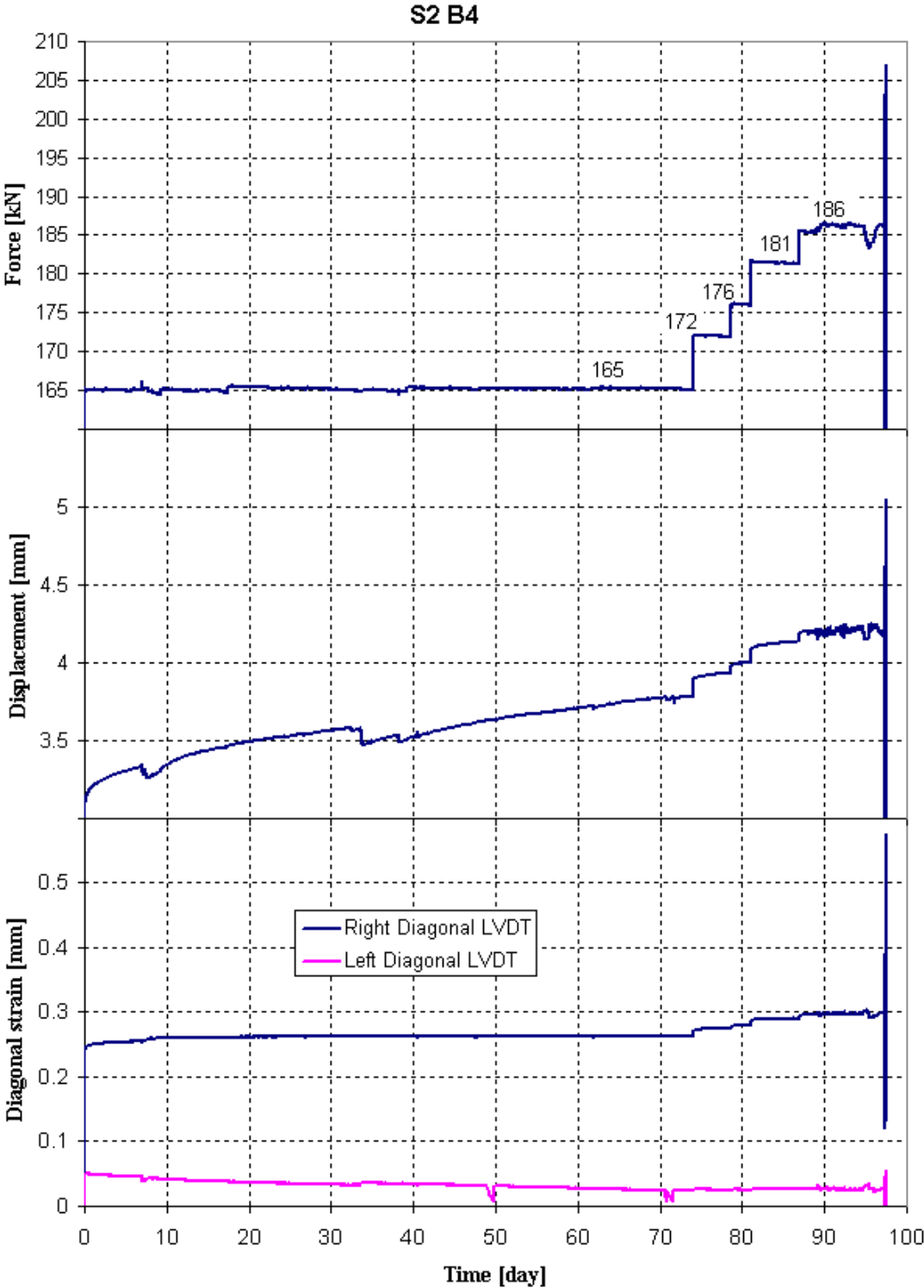

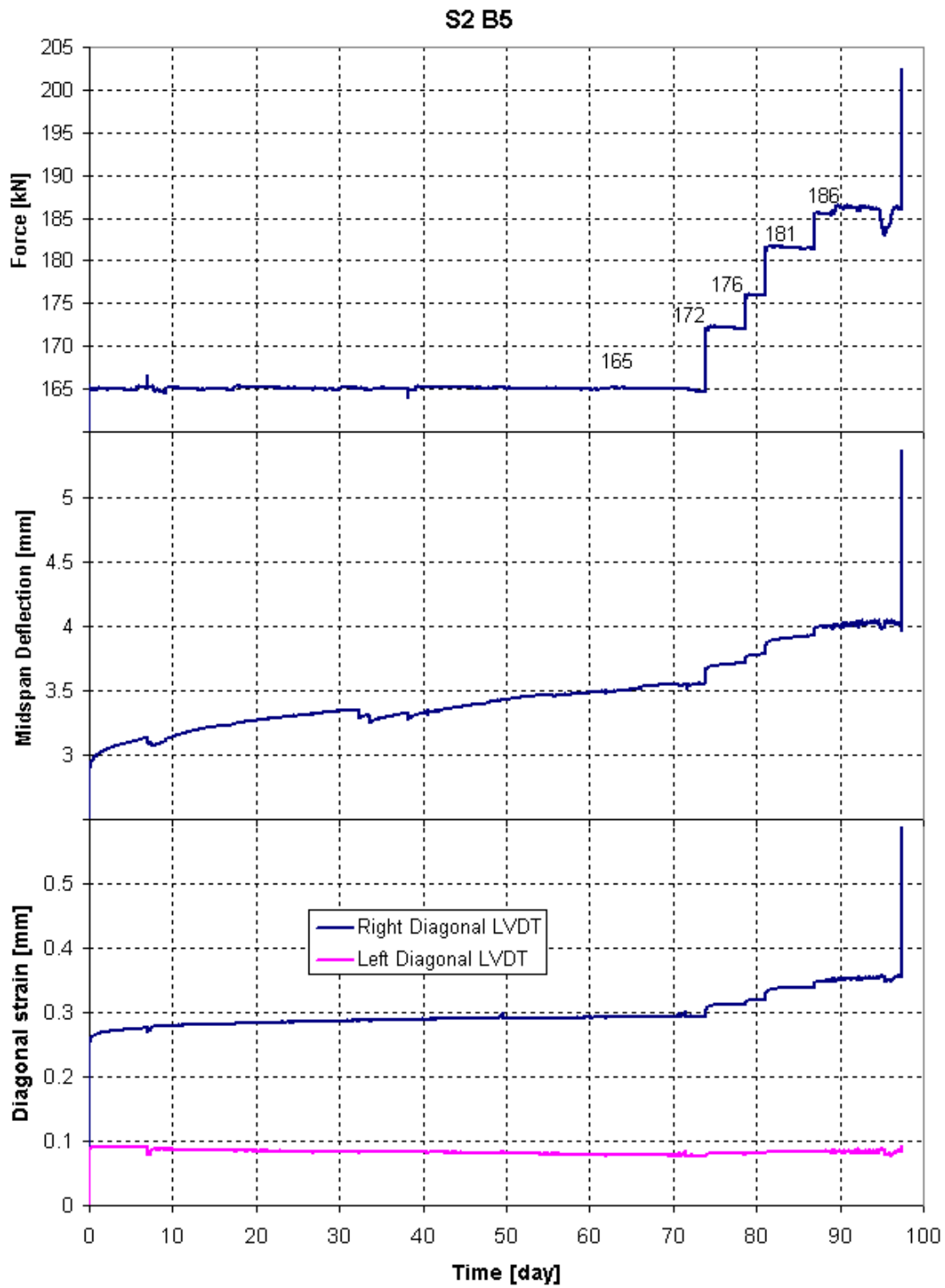**Fig. 47: Time-history of load, midspan and diagonal strain, Specimen S2B4**

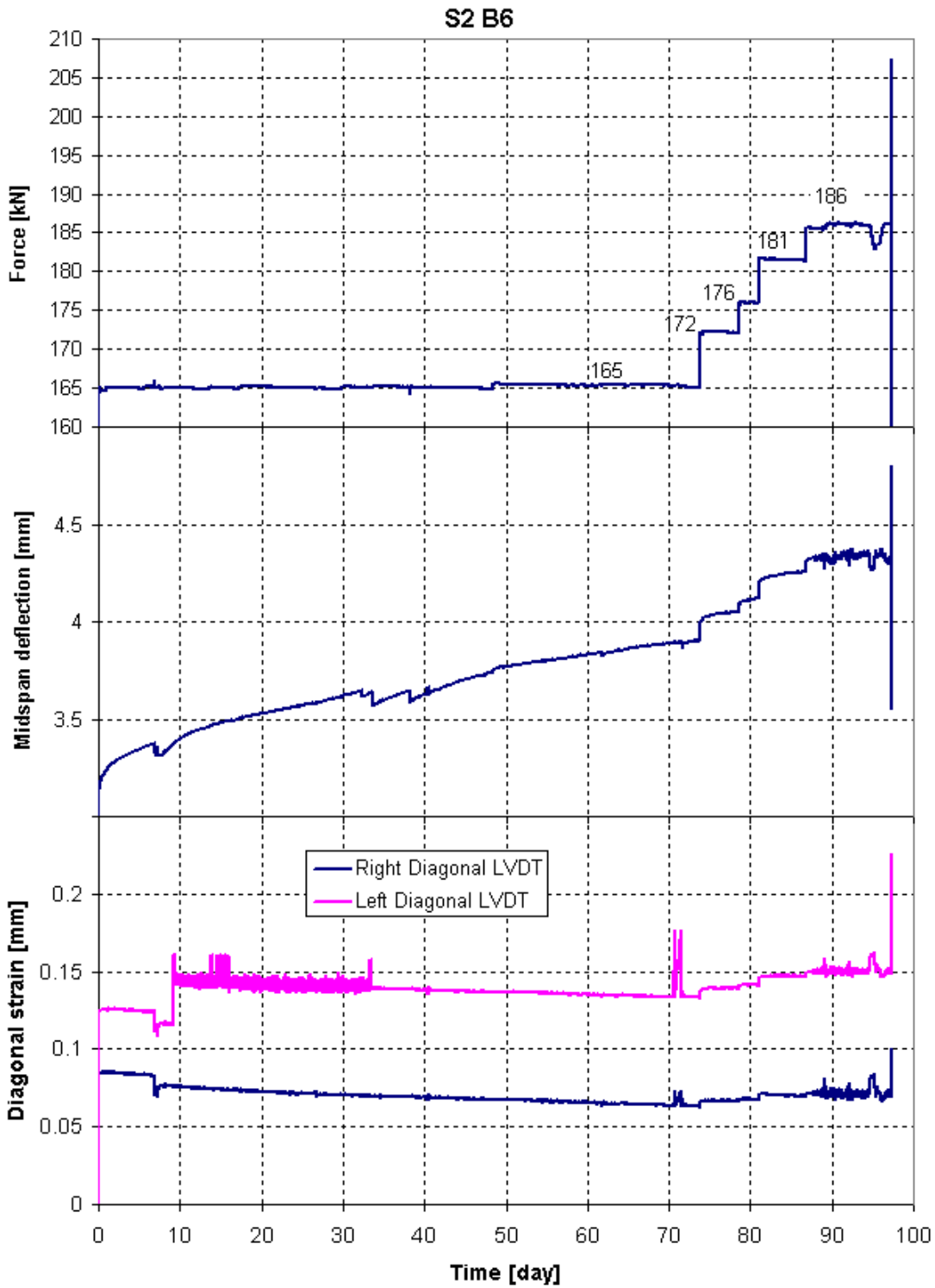**Fig. 48: Time-history of load, midspan and diagonal strain, Specimen S2B5**

Fig. 49: Time-history of load, midspan and diagonal strain, Specimen S2B6

6.4. Crack patterns

The crack patterns in the concrete beams are represented in Fig. 50 to Fig. 52. The crack patterns are obtained after various periods of time. The first monitoring of the cracks is performed just after loading in the same day. The most significant development of the crack pattern occurs in the first day of loading. In the figures below, the red cracks are new cracks observed at the indicated time during the sustained loading period.

The last figure is the crack pattern after failure. Hence, some of the bending cracks shown in this figure occur due to large deformation of the beam after failure. In the last figure, the cracks which cause failure are shown in a more pronounced way; the pronounced cracks represent the shear failure cracks, semi-thick crack represents clearly visible wide cracks which could have caused the shear failure, and thin cracks are the cracks which are barely visible. As mentioned in section 5.3, it is tried to mark the shrinkage cracks before the tests. These cracks are not drawn in the crack pattern, but some of the thin cracks appear during the test due to both shrinkage and loading stresses and it is hard to distinguish them from the bending and shear cracks. So, these cracks are shown in the figures. The blue dashed-dot lines and the green lines are representing the position of the longitudinal reinforcement and the position of the diagonal LVDT's, respectively.

One noticeable observation is that the failure crack does not necessarily follow the existing shear cracks. This behaviour can be seen e.g. in Fig. 50.
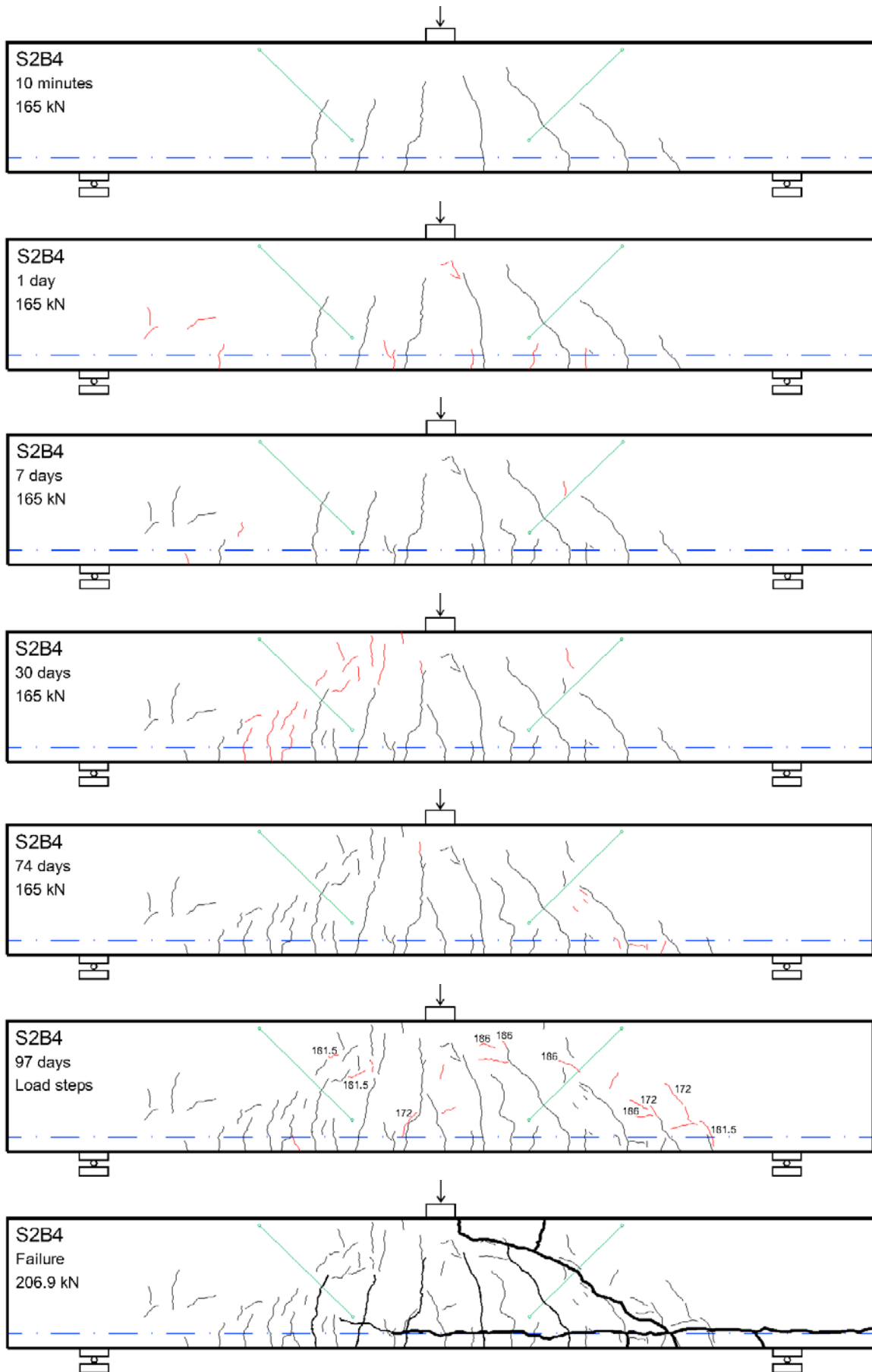
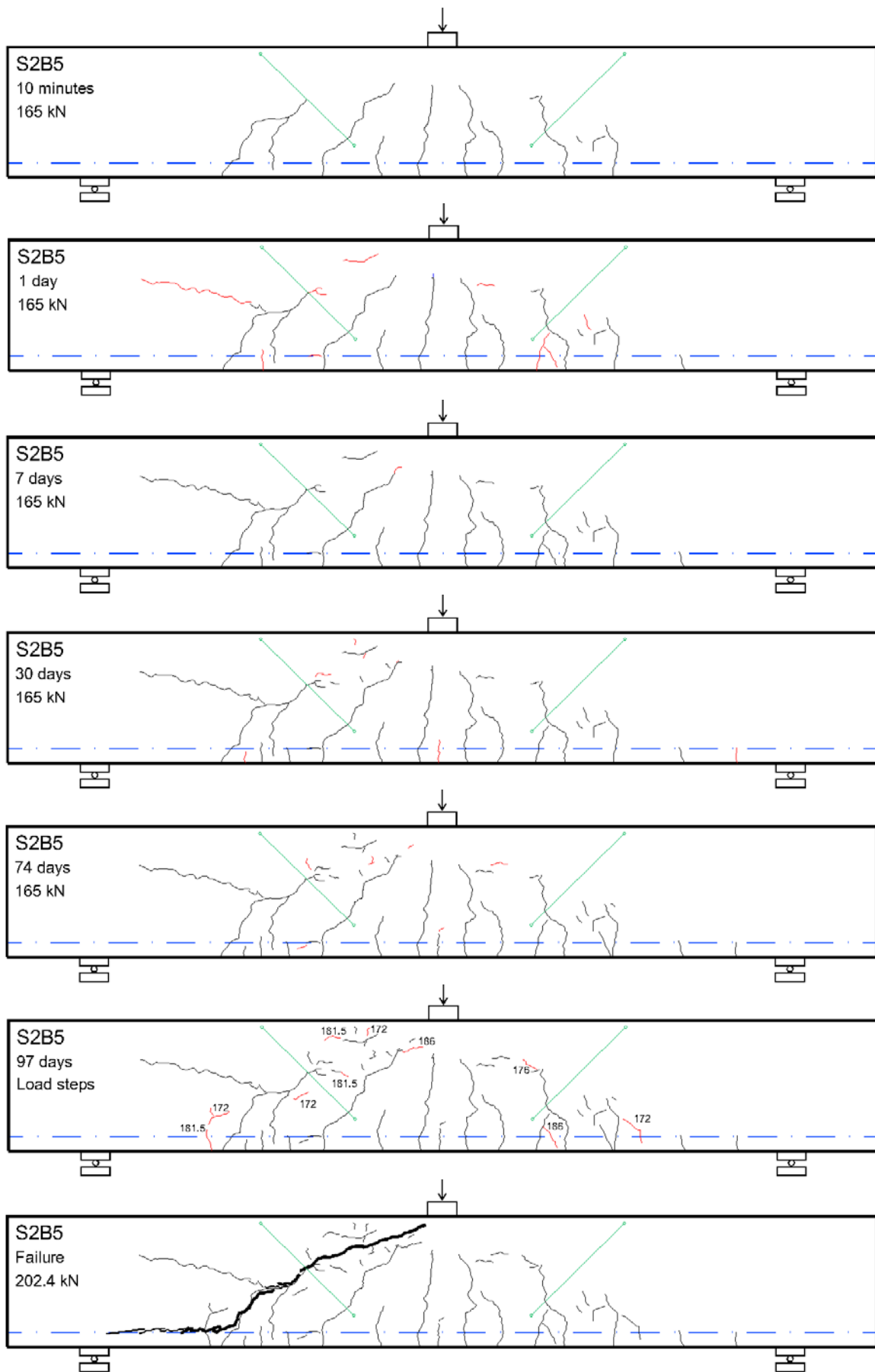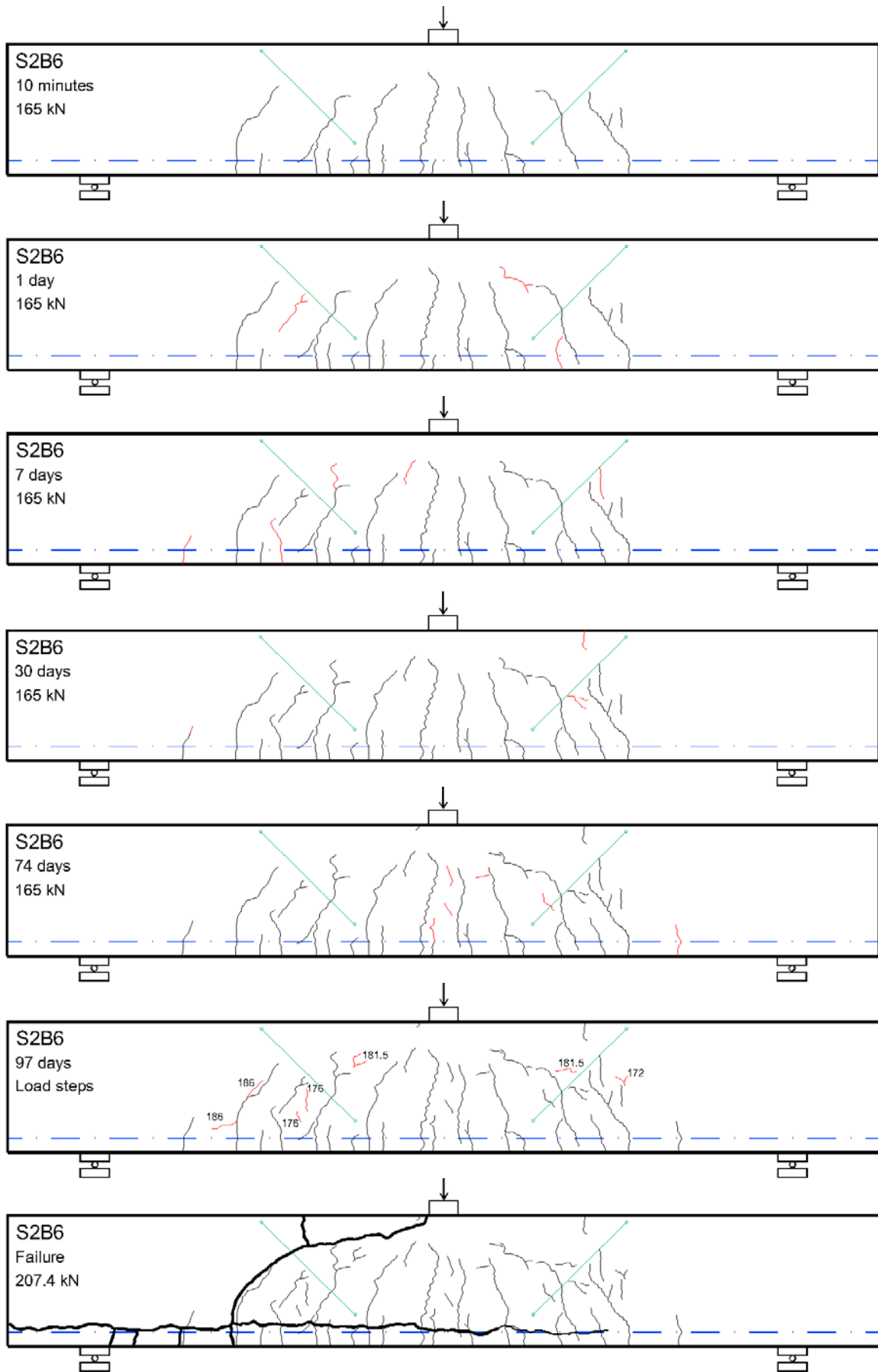**Fig. 50: Crack pattern in beam S2B4 during time**

Fig. 51: Crack pattern in beam S2B5 during time

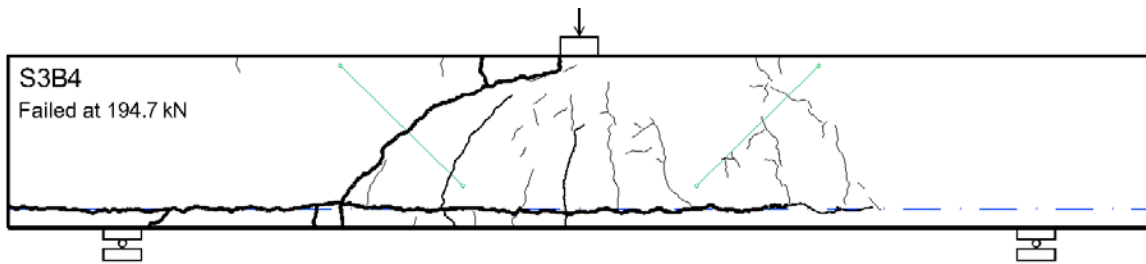**Fig. 52: Crack pattern in beam S2B6 during time**

Fig. 53: Crack pattern in specimen S3B4
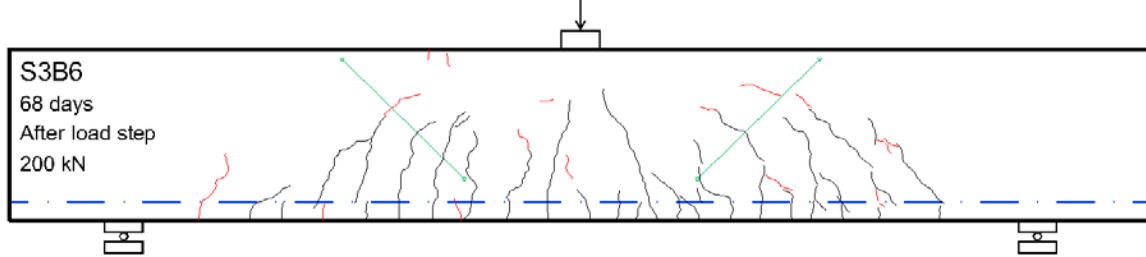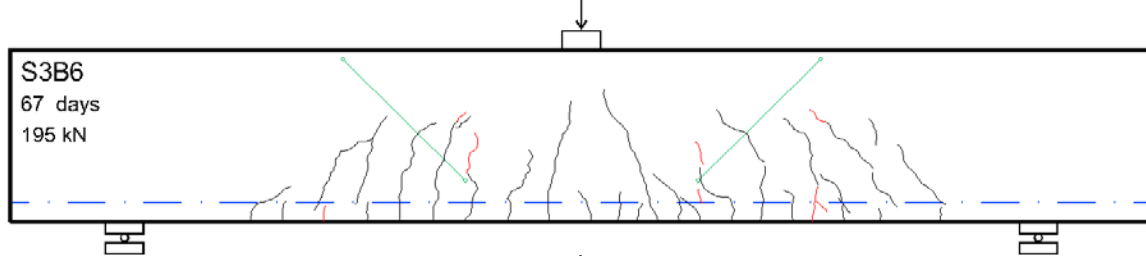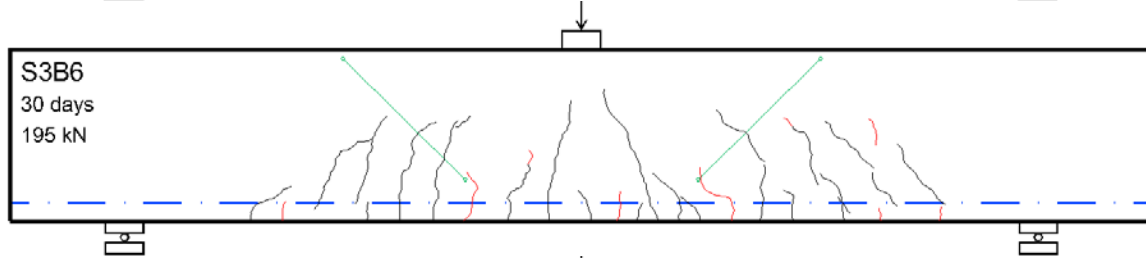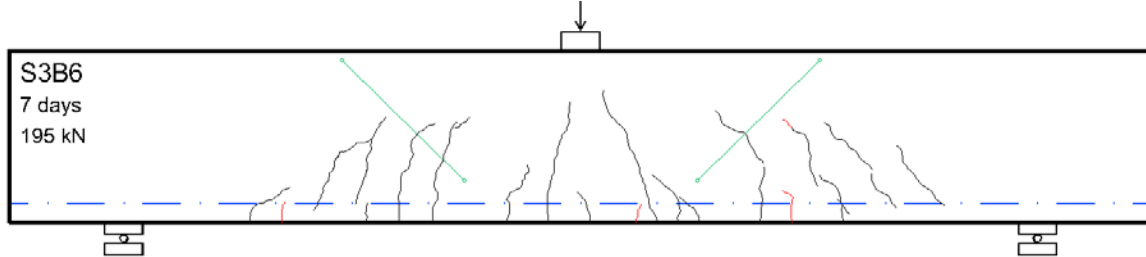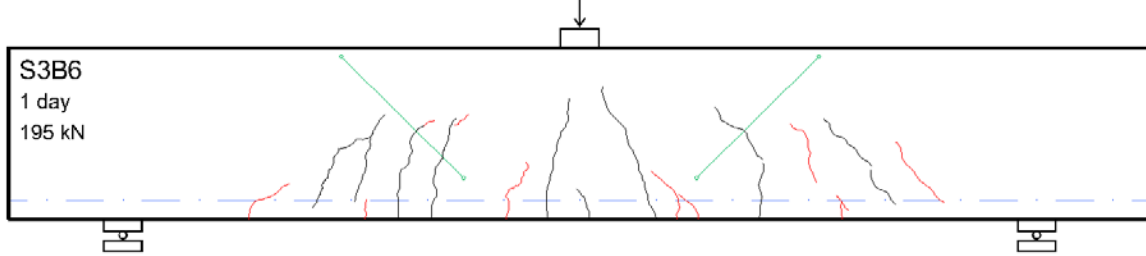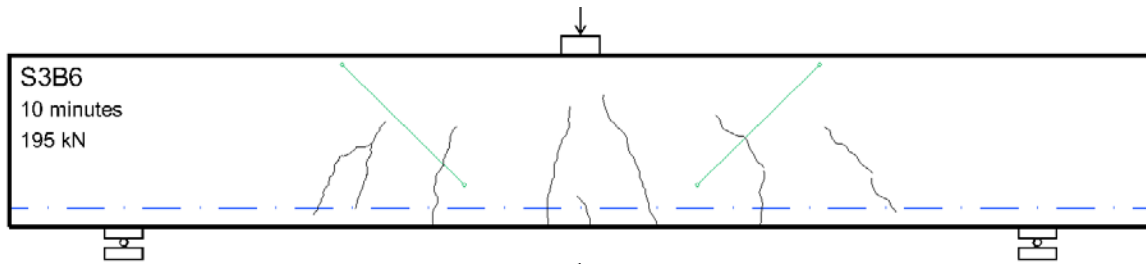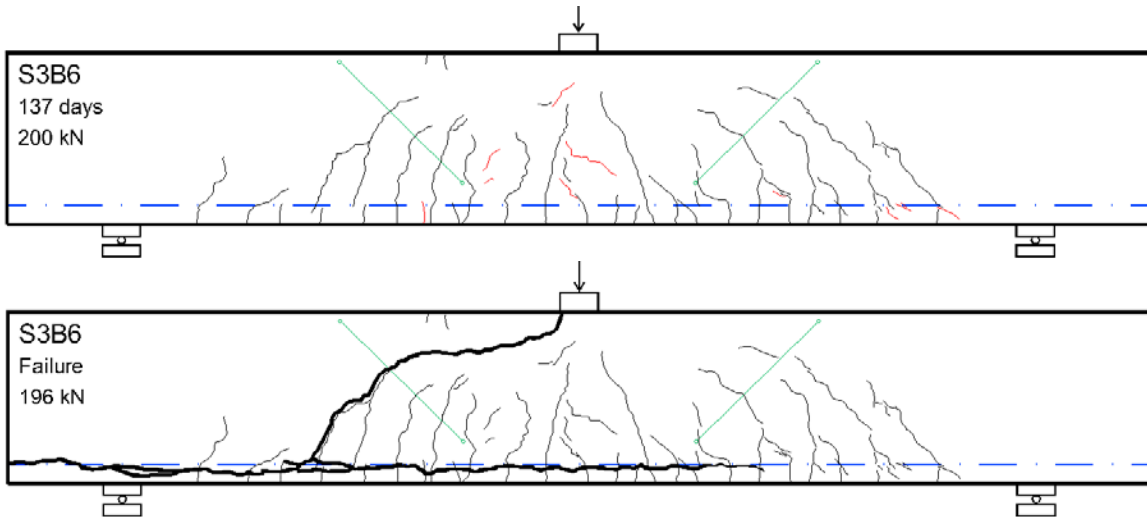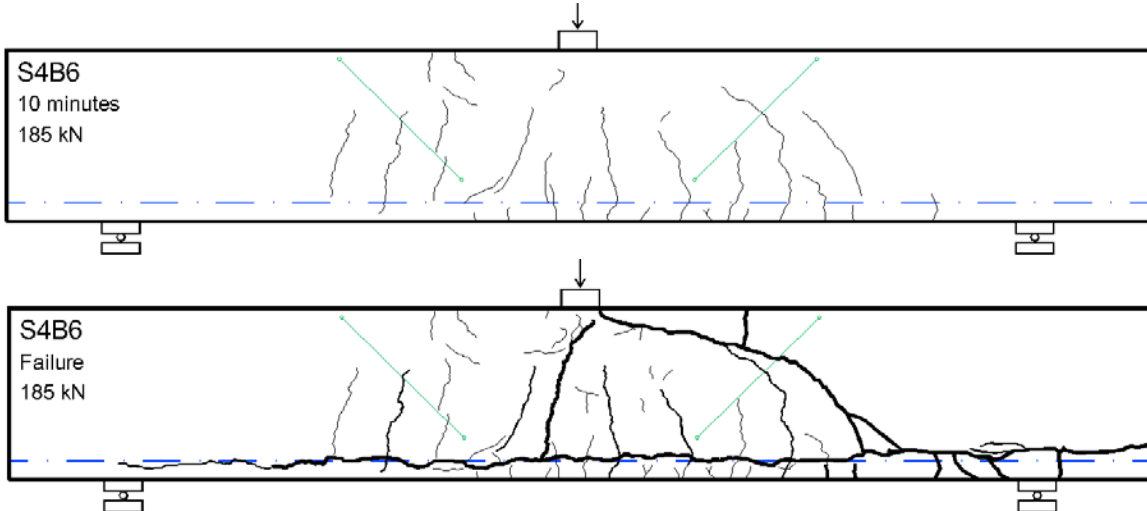
Fig. 54: Crack pattern in beam S3B6 during time

Fig. 55: Crack pattern in beam S4B6 during time
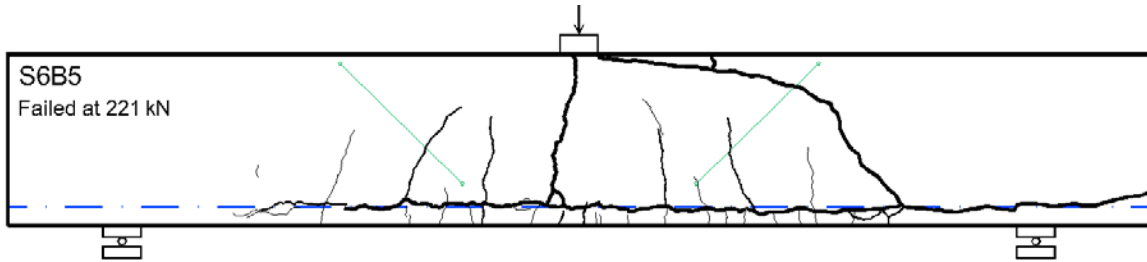

Fig. 56: Crack pattern in beam S6B5

6.5. Summary of long term-loading tests

Currently 4 series of beams specimens have been tested in long-term loading. Specimen S2B4, S2B5 and S2B6 out of series 2 were tested under a load equal to 87% of the ultimate short-term shear capacity for 74 days. After the 74 days sustained load test, the load was increased step by step to 97.5% of the ultimate capacity. When again no failure or growth in cracks was observed, the beams were loaded to failure. The ultimate capacities were about 7% higher than the mean short-term values and about 6% higher than the theoretically obtained value. A noticeable result is that during increasing the load level, some new cracks appeared on the beam but the main shear cracks did not grow anymore; only the width of the cracks (according to the diagonal LVDT's) increased.

Two beams out of series 3 were tested in long-term loading at a level of 95% of the mean short-term load. Specimen S2B4 failed just before reaching the 95% level. Beam specimen S2B5 and S2B6 were kept at 95% of ultimate short-term capacity, for 67 days. After this period, the load increased to 97% of theoretically obtained ultimate capacity at the corresponding time. This load level was kept for 70 days and after that the beams were unloaded for 50 days for changing the test setup. Beam S2B6 failed during reloading. The other beam is still loaded at 97% of estimated actual ultimate capacity.

The beams of series 4 were loaded at 95% of short-term ultimate capacity. Specimen S4B6 failed after 2.5 hours loading and specimens S2B4 and S2B5 are still in the setup. After 70 days of sustained loading, the strength of the concrete was increased due to further hydration and the ultimate shear capacity is theoretically obtained using Rafla's formula, then load was adjusted to 95% of the theoretically obtained ultimate capacity. No failure occurred in S2B4 and S2B5 after 6 months of sustained loading.

The beams of series 6 with high strength concrete (f_{cm} = 78 MPa) were loaded at 90% of ultimate shear capacity obtained in short-term tests. One of the beams failed during loading (S2B5) at 88.4% of mean short-term capacity and beams S2B4 and S2B6 are still under the sustained load.

Based on the results obtained from the sustained loading tests and short-term loading tests, reaching the maximum deflection possibly takes a couple of months due to creep effects in the concrete beam but the maximum crack width was reached within a couple of hours and if the beam resists the load in this period, it would probably resist "forever". Apparently in long-term loading, the shrinkage and stress relaxation influence on crack width and consequently the shear resistance increases.

Specimen S4B6 is the only sample which failed in sustained loading, even though the duration of the loading was not too long and probably the load was too close to the ultimate capacity of the beam. However, this sample shows that when the load level is close enough to the ultimate capacity, the beam will fail and this failure may happen within a few hours.

7. Conclusions

Based on the results of 15 short-term tests and 15 long-term tests the following provisional conclusions can be drawn:

- Long-term loading under 90-95% of ultimate capacity at constant humidity and temperature up to 6 months did not cause failure of the beam.

- Concrete beams without shear reinforcement present a brittle behaviour. This behaviour is more or less the same in NSC and HSC beams.

- The failure crack is not necessarily originates from the existing shear cracks

- Failure of the beam under sustained loads can occur within a couple of hours, but only the sustained load is very close to the short-term shear capacity.

- During long-term loading, due to creep effect, the deflection of the beam increases but it does not lead to failure.

- During long-term loading, unlike the length of the crack, the width of the crack does not increase and could even decrease. This phenomenon could be caused by stress relaxation and shrinkage effect.

- New cracks appear in the beam during long-term loading, but some main shear cracks do not propagate anymore.

8. References

[1]   Design and Control of Concrete Mixtures, Portland Cement Association (PCA), Old Orchard Road, Skokie, 1994.

Appendix I: Sieve analysis and concrete mix

Table 17. Sieve analysis of concrete, cast 1

Sieve	Sand 0-2	Sand 0-4	Gravel 4-16	Mixture Percentage
16 mm	0.0%	0.0%	3.7%	2.0%
8 mm	0.0%	0.0%	61.0%	32.7%
4 mm	0.0%	2.8%s	94.7%	52.0%
2 mm	0.0%	16.9%	98.5%	60.6%
1 mm	0.0%	31.6%	99.5%	68.0%
500 µm	0.6%	30.7%	100%	81.7%
250 µm	22.1%	89.8%	100%	95.3%
125 µm	91.9%	99.1%	100%	99.6%
63 µm	100%	100%	100%	100%
Fineness modulus	1.15%	3.01	6.57	4.92
Moisture	3.0%	4.0%	2.0%	
Fraction	0.0%	46.4%	53.6%	

Table 18. Mix proportions of the concrete per m³, cast 1

Component	Wet	Dry
CEM III/B 42.5 N LH/HS NA	330 kg	330 kg
Sand 0-2 mm	0 kg	0 kg
Sand 0-4 mm	868 kg	835 kg
Gravel 4-16 mm	982 kg	963 kg
PL BV-1M	0.495 kg	0.495 kg
Super plasticizer SPL VC 1550	0.660 kg	0.660 kg
Water	141 kg	194 kg
Air	15 L	15 L
Total	2322 kg	

Table 19. Sieve analysis of concrete, cast 2

Sieve	Sand 0-4	Sand 0-2	Gravel 4-16	Mixture Percentage
16 mm	0.0%	0.0%	58.8%	1.2%
8 mm	0.0%	0.0%	91.5%	30.1%
4 mm	4.2%	0.0%	99.0%	48.9%
2 mm	18.6%	0.0%	99.8%	59.8%
1 mm	34.6%	0.0%	100%	68.0%
500 μm	61.3%	0.6%	100%	81.1%
250 μm	89.8%	22.1%	100%	95.0%
125 μm	99.4%	91.9%	100%	99.7%
63 μm	100%	100%	100%	100%
Fineness modulus	3.08	1.15	6.51	4.84
Moisture	4.0%	3.0%	2.0%	
Fraction	48.8%	0.0%	51.2%	

Table 20. Mix proportions of the concrete per m³, cast 2

Component	Wet	Dry
CEM III/B 42.5 N LH/HS NA	330 kg	330 kg
Sand 0-4 mm	915 kg	880 kg
Sand 0-2 mm	0 kg	0 kg
Gravel 4-16 mm	942 kg	924 kg
Water	135	189
Air	15 L	15 L
Total	2323 kg	

Table 21. Sieve analysis of concrete, cast 3

Sieve	Sand 0-4	Sand 0-2	Gravel 4-16	Mixture Percentage
16 mm	0.0%	0.0%	1.9%	1.0%
8 mm	0.0%	0.0%	56.5%	30.5%
4 mm	4.2%	0.0%	91.1%	51.1%
2 mm	16.8%	0.0%	98.9%	61.1%
1 mm	30.9%	0.0%	99.7%	68.0%
500 μm	64.2%	0.6%	100%	83.5%
250 μm	90.2%	22.1%	100%	95.5%
125 μm	99.7%	91.9%	100%	99.9%
63 μm	100%	100%	100%	100%
Fineness modulus	3.06	1.15	6.48	4.90
Moisture	4.0%	3.0%	2.0%	
Fraction	46.1%	0.00%	53.9%	

Table 22. Mix proportions of the concrete per m^3, cast 3

Component	Wet	Dry
CEM III/B 42.5 N LH/HS NA	330 kg	330 kg
Sand 0-4 mm	865 kg	831 kg
Sand 0-4 mm	0 kg	0 kg
Gravel 4-16 mm	992 kg	972 kg
Super plasticizer SPL VC 1550	0.594 kg	0.594 kg
Water	136 kg	189 kg
Air	15 L	15 L
Total	2323 kg	

Table 23. Sieve analysis of concrete, cast 4

Sieve	Sand 0-4	Sand 0-2	Gravel 4-16	Mixture Percentage
16 mm	0.0%	0.0%	2.3%	1.2%
8 mm	0.0%	0.0%	57.5%	31.0%
4 mm	7.0%	0.0%	95.8%	54.9%
2 mm	12.1%	0.0%	99.0%	59.0%
1 mm	30.9%	0.0%	99.7%	68.0%
500 μm	53.3%	0.6%	100%	78.5%
250 μm	90.5%	22.1%	100%	95.6%
125 μm	99.0%	91.9%	100%	99.5%
63 μm	100%	100%	100%	100%
Fineness modulus	2.93	1.15	6.54	4.88
Moisture	4.0%	3.0%	2.0%	
Fraction	46.1%	0.0%	53.9%	

Table 24. Mix proportions of the concrete per m³, cast 4

Component	Wet	Dry
CEM III/B 42.5 N LH/HS NA	330 kg	330 kg
Sand 0-4 mm	864 kg	831 kg
Sand 0-4 mm	0 kg	0 kg
Gravel 4-16 mm	993 kg	973 kg
Super plasticizer SPL VC 1550	0.596 kg	0.594 kg
Water	136 kg	189 kg
Air	15 L	15 L
Total	2323 kg	

Table 25. Sieve analysis of concrete, cast 5

Sieve	Sand 0-4 Type I (Grensmaas)	Sand 0-4 Type II	Sand 0-2	Gravel 4-16	Mixture Percentage
16 mm	0.0%	0.0%	0.0%	0.6%	0.3%
8 mm	0.0%	0.0%	0.0%	51.5%	27.8%
4 mm	1.7%	2.0%	0.0%	86.5%	47.4%
2 mm	14.1%	13.6%	0.0%	98.9%	59.5%
1 mm	35.7%	28.4%	0.0%	99.9%	68.0%
500 μm	60.8%	56.9%	0.6%	100%	80.7%
250 μm	89.8%	92.5%	22.1%	100%	96.1%
125 μm	99.3%	99.8%	91.9%	100%	99.8%
63 μm	100%	100%	100%	100%	100%
Fineness modulus	3.01	2.93	1.15	6.38	4.80
Moisture	4.0%	4.0%	3.0%	2.0%	
Fraction	16.2%	30.1%	0.0%	53.7%	

Table 26. Mix proportions of the concrete per m^3, cast 5

Component	Wet	Dry
CEM III/B 42.5 N LH/HS NA	320 kg	320 kg
Sand 0-4 mm Type I	304 kg	292 kg
Sand 0-4 mm Type II	565 kg	543 kg
Sand 0-2 mm	0 kg	0 kg
Gravel 4-16 mm	990 kg	970 kg
Water	142 kg	195 kg
Air	15 L	15 L
Total	2321 kg	

Table 27. Sieve analysis of concrete, cast 6

Sieve	Sand 0-4 Type I (Grensmaas)	Sand 0-4 Type II	Gravel 4-16	Mixture Percentage
16 mm	0.0%	0.0%	5.5%	3.0%
8 mm	0.0%	0.0%	51.8%	27.9%
4 mm	1.8%	5.1%	92.1%	51.4%
2 mm	13.0%	15.7%	99.0%	59.8%
1 mm	34.6%	19.1%	99.7%	68.0%
500 µm	60.9%	54.9%	100%	81.0%
250 µm	88.5%	91.3%	100%	95.5%
125 µm	99.3%	99.2%	100%	99.6%
63 µm	100%	100%	100%	100%
Fineness modulus	2.98	2.97	6.48	
Moisture	4.0%	4.0%	2.0%	
Fraction	16.2%	30.0%	53.8%	

Table 28. Mix proportions of the concrete per m³, cast 6

Component	Wet	Dry
CEM I 52.5 R Deuna	280 kg	280 kg
CEM III/B 42.5 N LH/HS NA	145 kg	145 kg
Sand 0-4 mm Type I	282 kg	271 kg
Sand 0-4 mm Type II	523 kg	503 kg
Gravel 4-16 mm	920 kg	902 kg
Fly ash	60 kg	60 kg
Super Plasticizer SPL VC 1550	3.686 kg	3.686 kg
Delayer VTR VZ 1	0.97 kg	0.97 kg
Water	122 kg	171 kg
Air	15 L	15 L
Total	2336 kg	

Table 29. Sieve analysis of concrete, cast 7

Sieve	Mixture Percentage
16 mm	2.9%
8 mm	27.6%
4 mm	52.4%
2 mm	60.8%
1 mm	79.8%
500 μm	95.8%
250 μm	99.7%
125 μm	100%
63 μm	100%

Table 30. Mix proportions of the concrete per m³, cast 7

Component	Wet	Dry
CEM I 52.5 R Deuna	280 kg	280 kg
CEM III/B 42.5 N LH/HS NA	145 kg	145 kg
Sand 0-4 mm Type I	288 kg	277 kg
Sand 0-4 mm Type II	535 kg	515 kg
Gravel 4-16 mm	919 kg	901 kg
Fly ash	60 kg	60 kg
Super Plasticizer SPL VC 1550	2.91 kg	2.91 kg
Delayer VTR VZ 1	0.97 kg	0.97 kg
Water	115 kg	165 kg
Air	15 L	15 L
Total	2347 kg	

Appendix II: Analysis of specimen series 1-5

Cover
*<BS EN 1992–1–2: Tables 5.8, 5.9, 5.10, 5.11> **Error! Reference source not found.***
Nominal cover, c_{nom}

$c_{nom} = c_{min} + \Delta c_{dev}$
where
$c_{min} = \max[c_{min,b}; c_{min,dur}]$
where
$c_{min,b}$ = minimum cover due to bond
= diameter of bar.
Assume 20 mm main bars
$c_{min,dur}$ = minimum cover due to environmental conditions.
Assuming XC3 (moderate humidity or cyclic wet and
dry) and secondarily XF1 (moderate water saturation
without de-icing salt) using C30/37 concrete
$c_{min,dur}$ = 25 mm
Δc_{dev} = allowance in design for deviation. Assuming no measurement
of cover Δc_{dev} = 5 mm
$\therefore c_{nom} = 25 + 5 = 30$ mm

Fire:

<BS EN 1992-1-2, 5.6.3(1), Table 5.6>
Check adequacy of section for 90 minutes fire resistance (i.e. $R = 90$)
For $b_{min} = 200$ mm, minimum axis distance, $a = 45$ mm $\therefore$ OK

$c_{nom} = 30$ mm

Effective Depth

$d = 450 - 30 - 20 / 2 = 410$ mm

Shear Capacity

<Rafla's formula>
$\tau_c = 0.29 \, \alpha_u \, \alpha_h \, (f_{cm})^{1/2} \, (\rho)^{1/3}$
where,
$\alpha_u = 0.795 + 0.293 \, (3.5 - a/d)^{2.5}$ for $2.0 \leq a/d \leq 3.5$
$a/d = 1200/410 = 2.92$
$\therefore \alpha_u = 0.795 + 0.293 \, (3.5 - 2.92)^{2.5} = 0.87$
$\alpha_h = 1/(d/100)^{1/4} = 1/(410/100)^{1/4} = 0.7027$
$f_{cm} = 35$ Mpa (Cube test)
$\rho = 1.047$
$\therefore \tau_c = 0.29 \, \alpha_u \, \alpha_h \, (f_{cm})^{1/2} \, (\rho)^{1/3} = 0.29 \, (0.87) \, (0.7027) \, (35)^{1/2} \, (1.047)^{1/3}$

$\tau_c = 1.07$ N/mm^2

Shear Resistance,

$V_{Rd} = \tau_c \, b \, d$
where,

τ_c = shear capacity = 1.07 N/mm^2
b = width of the beam = 200 mm
d = effective depth = 410 mm
$\therefore V_{Rd} = 87.7 \times 10^3$ N

Upper Confidence Limit (UCL) of Shear Resistance
$V_{Rd,0.95} = V_{RD} (1 + \lambda . SD)$
where,
$\lambda = 1.64$
$SD = 0.12$
$\therefore V_{Rd,0.95} = 87740 (1 + 1.64 \times 0.12) = 105 \times 10^3$ N

Ultimate bond stress
$f_{bd} = 2{,}25 \, \eta_1 \eta_2 f_{ctd}$
where,
$\eta_1 = 1.0$ when the 'good' condition is obtained
$\eta_2 = 1.0$ for $\emptyset < 32$
f_{ctd} = the design value of the tensile strength
= $\alpha_{ct} f_{ctk,0,05} / \gamma_c$
$f_{ctk,0,05} = 2.0$ (for $f_{ck} = 35$ MPa)
$\gamma_c = 1.5$
$\alpha_{ct} = 1$
$\therefore f_{ctd} = (1)(2.0) / (1.5) = 1.33$ MPa
$\therefore f_{bd} = 2{,}25 \, (1) \, (1) \, (1.33) = 3.0$ MPa

Anchorage
The basic required anchorage length $l_{b,rqd}$, for anchorage the force $A_s.\sigma_{sd}$ in a straight bar
assuming constant bond stress equal to f_{bd} follows from:
$l_{b,rqd} = (\emptyset/4)(\sigma_{sd}/f_{bd}) = (20/4)(\sigma_{sd}/3,0)$
where,
$f_{bd} = 3.0$ Mpa

σ_{sd} is the design stress of the bar at the position from where the anchorage is measured from.
$\sigma_{sd} = N_s / A_s$
where,
$N_s = R_{Ed} (450) / 410$
where,
$R_{Ed} = 1.5 V_{Rd,0.95} = 157.5 \times 10^3$ N
$\therefore N_s = 172.8 \times 10^3$ N
$\therefore \sigma_{sd} = 172.8 \times 10^3 / 942 = 183.5$ N/mm^2

$\therefore l_{b,rqd} = (20/4)(183.5/3) = 306$ mm

Analysis
Design moments
$M_{Ed} = V_{Rd,0.95} L /2 + w L^2/8$
where,
$V_{Rd,0.95} = 105 \times 10^3$ kN
L = 2.4 m

w = self-weight of the beam per meter = 2.25 kN/m

M_{Ed} = 127 kNm

Effective depth

$d = 450 - 30 - 20 / 2 = 410$ mm

Flexure in span

$K = M_{Ed} / b\, d^2 f_{ck} = 127 \times 10^6 / (200 \times 410^2 \times 35) = 0.1079$

$z / d = 0.9$

$z = 0.9 \times 410 = 369$

Stress in steel

$\sigma_s = f_{ck}\, b\, d\, [0.633 - (0.4 - 1.46\, K)^{1/2}] / A_s$

$= (35)(200)(410)[0.633 - (0.4 - 1.46 \times 0.1079)^{1/2}] / 942 = 425$ N/mm^2

Concrete Volume

Total volume = $30 \times 0.2 \times .45 \times 3 = 7.29$ m^3

Reinforcement

Total length = $30 \times 3 \times 3 = 270$ m

Steel weight = $270 \times 78\, \pi\, 0.01^2 = 6.62$ kN

Appendix III: FE Modelling in ATENA

Finite Element Modelling is performed in ATENA 2D version 4.1.1. The element type chosen for concrete is "3D Nonlinear Cementitious 2". This element type very appositely characterises the behaviour of concrete in terms of tension (the origination and propagation of tension cracks) and compression. It is based on the non-linear fracture mechanics and incorporates the reduction in the strength of the material after the origination of cracks. The main parameters of the 3D Nonlinear Cementitious 2 material are tensile strength and energy to fracture. A maximum element size of 37.5 mm is chosen for this element type. Meshes are refined around the loading plate and reinforcing bar, see Fig. 57. The material properties e.g. elastic modulus and fracture energy is calculated automatically by the software based on the cube compressive strength. Only the tensile strength is adjusted by the values obtained from test results.
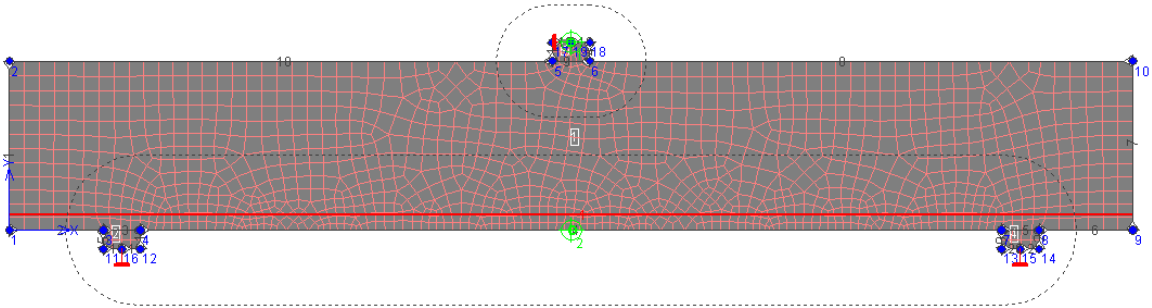

Fig. 57: FE Modelling of the beam in ATENA

"Reinforcement" and "Bond for Reinforcement" elements are used to model the reinforcing bars and the bond between bars and concrete, respectively. The material properties for reinforcement is; elastic modulus E=2.1E+05 MPa, yield strength σ_y=555.0 MPa for 20 mm diameter bars and 572.0 MPa for 25 diameter bars. For bond properties CEB-FIP Model Code 1990 is used with ribbed reinforcement, good bond quality and confined concrete is

To model the loading plate and supports, "Plane Stress Elastic Isotropic" element is chosen.

Newton – Raphson method was used for the solution in ATENA 2D.